NPL
National Physical Laboratory

dti

A NATIONAL MEASUREMENT GOOD PRACTICE GUIDE

No. 52

Determination of Residual Stresses by X-ray Diffraction - Issue 2

dti

The DTI drives our ambition of 'prosperity for all' by working to create the best environment for business success in the UK. We help people and companies become more productive by promoting enterprise, innovation and creativity.

We champion UK business at home and abroad. We invest heavily in world-class science and technology. We protect the rights of working people and consumers. And we stand up for fair and open markets in the UK, Europe and the world.

This Guide was developed by the National Physical Laboratory on behalf of the NMS.

Measurement Good Practice Guide No. 52

Determination of Residual Stresses by X-ray Diffraction – Issue 2

M.E. Fitzpatrick[1], A.T. Fry[2], P. Holdway[3],
F.A. Kandil[2], J. Shackleton[4] and L. Suominen[5]
[1] Open University, [2] National Physical Laboratory, [3] QinetiQ,
[4] Manchester Materials Science Centre, [5] Stresstech Oy

Abstract:

This Guide is applicable to X-ray stress measurements on crystalline materials. There is currently no published standard for the measurement of residual stress by XRD. This Guide has been developed therefore as a source of information and advice on the technique. It is based on results from three UK inter-comparison exercises, detailed parameter investigations and discussions and input from XRD experts. The information is presented in separate sections which discuss the fundamental background of X-ray diffraction techniques, the different types of equipment that can be used, practical issues relating to the specimen, the measurement procedure itself and recommendations on how and what to record and report. The appendices provide further information on uncertainty evaluation and some recommendations regarding the data analysis techniques that are available. Where appropriate key points are highlighted in the text and summarised at the end of the document.

This second issue includes a new section on depth profiling, additional examples of uncertainty evaluation and recommendations regarding X-ray elastic constants and data presentation.

ISSN 1744-3911

September 2005

National Physical Laboratory
Teddington, Middlesex, United Kingdom, TW11 0LW
Website: www.npl.co.uk

Acknowledgements

This Guide has been produced as a deliverable in MPP8.5 – a *Measurements for Processability and Performance of Materials* project on the measurement of residual stress in components. The MPP programme was sponsored by the Engineering Industries Directorate of the Department of Trade and Industry. The advice and guidance from the programme's Industrial Advisory Group and XRD Focus Group are gratefully acknowledged.

The authors would like to acknowledge important contributions to this work from Jerry Lord, the enthusiasm of the XRD Focus Group established for this project and all participants of the XRD Round Robin exercises.

For further information on X-ray diffraction or *Materials Measurement* contact Tony Fry or the Materials Enquiry Point at the National Physical Laboratory:

Tony Fry
Tel: 020 8943 6220
Fax: 020 8943 6772
E-mail: tony.fry@npl.co.uk

Materials Enquiry Point
Tel: 020 8943 6701
Fax: 020 8943 7160
E-mail: materials@npl.co.uk

Contents

1 Introduction

In measuring residual stress using X-ray diffraction (XRD), the **strain** in the crystal lattice is measured and the associated **residual stress** is determined from the elastic constants assuming a linear elastic distortion of the appropriate crystal lattice plane. Since X-rays impinge over an area on the sample, many grains and crystals will contribute to the measurement. The exact number is dependent on the grain size and beam geometry. Although the measurement is considered to be near surface, X-rays do penetrate some distance into the material: the penetration depth is dependent on the anode, material and angle of incidence. Hence the measured strain is essentially the average over a few microns depth under the surface of the specimen.

At the time of publishing there are no published standards for the measurement of residual stress by XRD. The first issue of this guide was used to provide UK input into the European Standard being prepared by CEN TC 138/WG 10 "X-ray Diffraction". This second issue of the Measurement Good Practice Guide has been developed based on continued work from inter-comparison exercises, detailed parameter investigations and discussions conducted with XRD experts within Focus Groups to offer additional advice on good measurement practice.

This document contains additional advice and examples relating to depth profiling and uncertainty evaluation with regards to XRD measurements for the evaluation of residual stress in components. It is broken down into sections which discuss the fundamental background of X-ray diffraction techniques, the different types of equipment that can be used, practical issues relating to the specimen, the recommended measurement procedure and recommendations on how and what to record and report. The appendices provide further information on uncertainty evaluation and some recommendations regarding the data analysis techniques that are available.

2 Scope

This Measurement Good Practice Guide describes a recommended practice for measuring residual strains using X-ray diffraction. The method is non-destructive and is applicable to crystalline materials with a relatively small or fine grain size. The material may be metallic or ceramic, provided that a diffraction peak of suitable intensity, and free of interference from neighbouring peaks, can be produced.

The recommendations are meant for stress analysis where only the ***peak shift*** is determined. If a full triaxial analysis of stress is performed, using a stress-free reference, then the absolute peak location has to be determined. However, such an analysis is beyond the scope of this Guide, which assumes that measurements are made with the assumption that the stress normal to the surface is zero i.e. **plane stress conditions**, and so a full triaxial analysis is not required.

If measurements are performed which are outside of the scope of this document then the user should be aware that additional complexities are likely to occur, and extreme caution should be exercised with regards to experimental procedure and subsequent data analysis and interpretation.

In all instances it is recommended that the user consult with the manufacturer's guide in association with this document.

During the measurement, the user is responsible for adhering to the relevant safety procedures for ionising radiations imposed by Law.

3 Definitions

Normal Stress

Normal stress is defined as the stress acting normal to the surface of a plane; the plane on which these stresses are acting is usually denoted by subscripts. For example consider the general case as shown in Figure 3.1, where stresses acting normal to the faces of an elemental cube are identified by the subscripts that also identify the direction in which the stress acts,

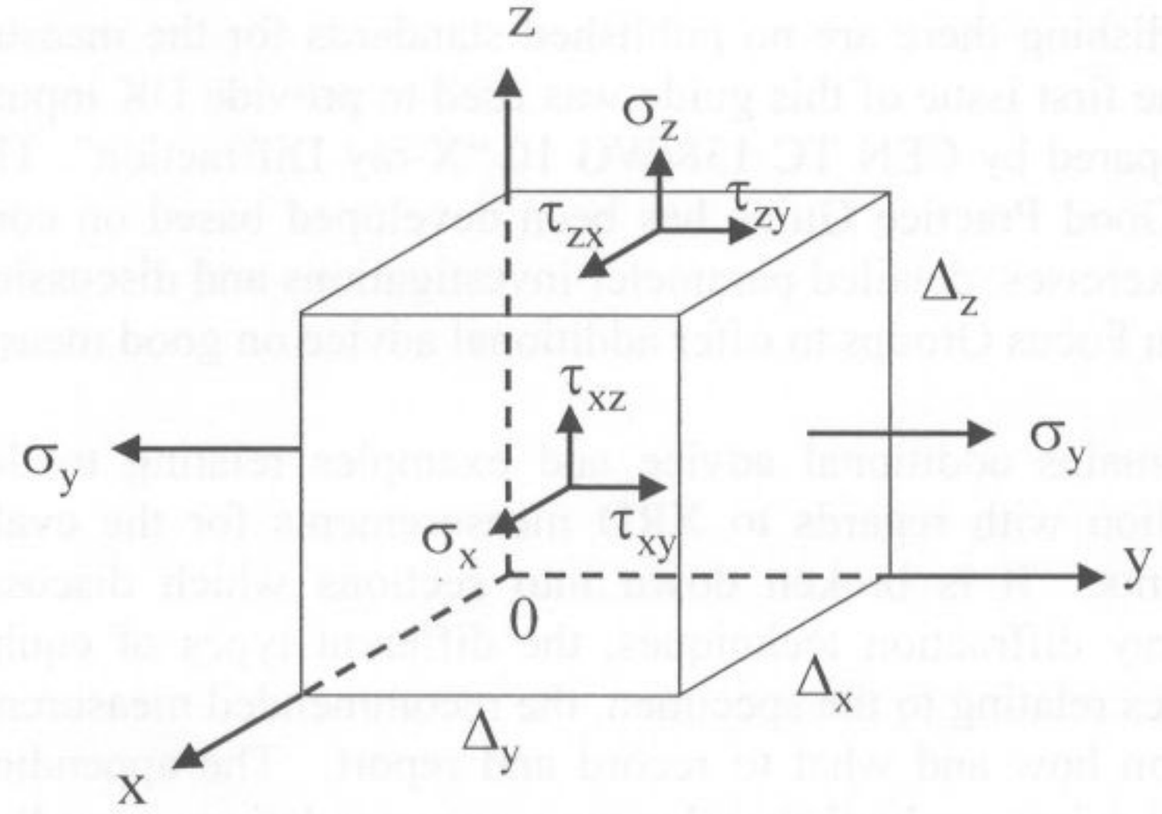

Figure 3.1 Stresses acting on an elemental unit cube.

e.g. σ_x is the normal stress acting in the x direction. Since σ_x is a normal stress it must act on the plane perpendicular to the x direction. The convention used is that positive values of normal stress denote tensile stress, and negative values denote a compressive stress.

Shear Stress

A shear stress acts perpendicular to the plane on which the normal stress is acting. Two subscripts are used to define the shear stress, the first denotes the plane on which the shear stress is acting and the second denotes the direction in which the shear stress is acting. Since a plane is most easily defined by its normal, the first subscript refers to this. For example, τ_{zx} is the shear stress on the plane perpendicular to the z-axis in the direction of the x-axis. The sign convention for shear stress is shown in Figure 3.2, which follows Timoshenko's notation. That is, a shear stress is positive if it points in the positive direction on the positive face of a unit cube. It is negative if it points in the negative direction of a positive face. All of the shear stresses in (a) are positive shear stresses regardless of the type of normal stresses that are present, likewise all the shear stresses in (b) are negative shear stresses.

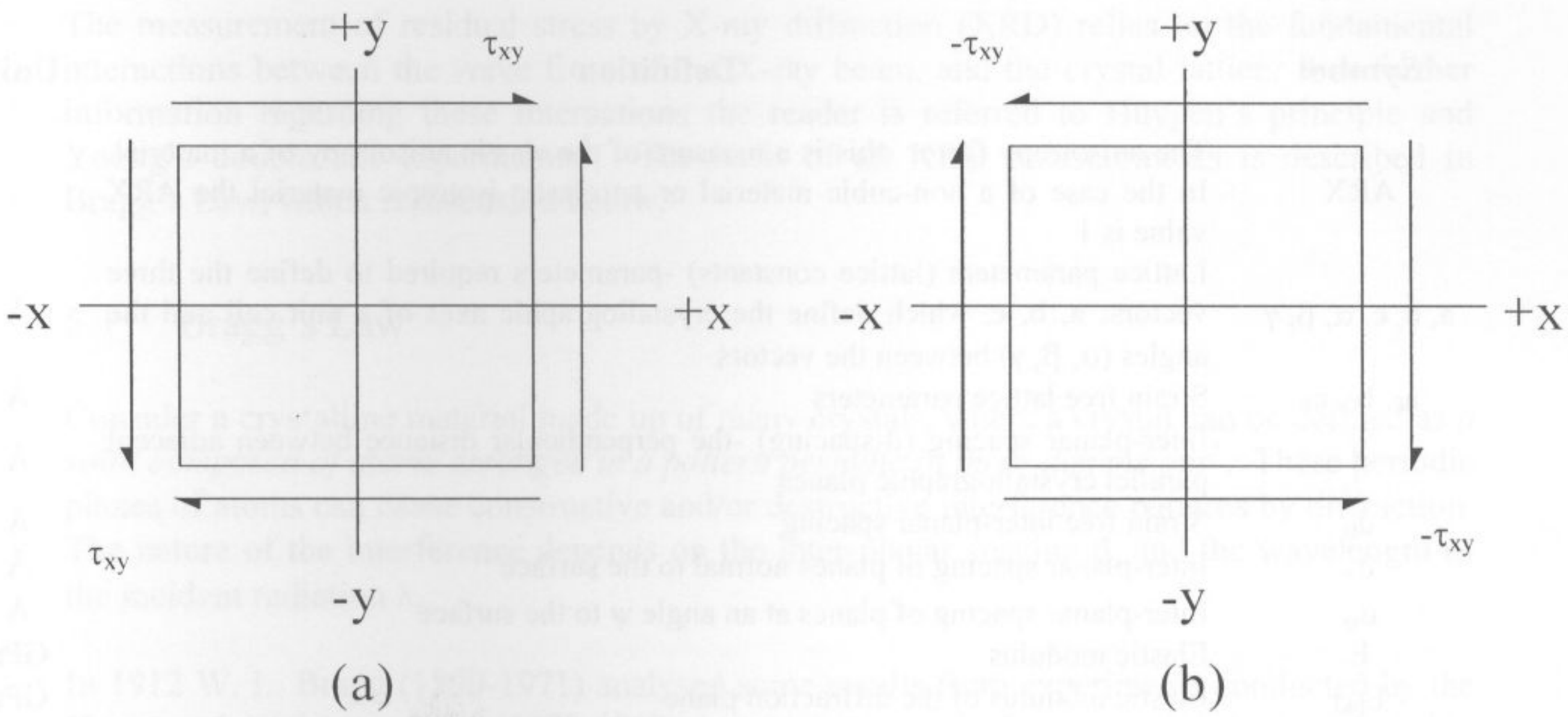

Figure 3.2 Sign convention for shear stress - (a) Positive, (b) negative.

Principal Stress

Principal stresses are those stresses that act on the 'principal planes'. For any state of stress it is possible to define a coordinate system, which has **axes perpendicular to the planes** on **which only normal stresses act** and on **which no shear stresses act.** These planes are referred to as the principal planes. In the case of two-dimensional plane stress there are two principal stresses σ_1 and σ_2. These occur perpendicular to each other, and by convention σ_1 is algebraically the largest. The directions along which the principal stresses act are referred to as the principal axes 1, 2 and 3. The specification of the principal stresses and their direction provides a convenient way of describing the stress state at a point.

4 Symbols

Symbol	Definition	Units
ARX	The anisotropy factor -this is a measure of the elastic anisotropy of a material. In the case of a non-cubic material or an elastic isotropic material the ARX value is 1	
a, b, c, α, β, γ	Lattice parameters (lattice constants) -parameters required to define the three vectors; **a**, **b**, **c**, which define the crystallographic axes of a unit cell and the angles (α, β, γ) between the vectors	Å
a_0, b_0, c_0	Strain free lattice parameters	Å
d	Inter-planar spacing (d-spacing) -the perpendicular distance between adjacent parallel crystallographic planes	Å
d_0	Strain free inter-planar spacing	Å
d_n	Inter-planar spacing of planes normal to the surface	Å
d_ψ	Inter-planar spacing of planes at an angle ψ to the surface	Å
E	Elastic modulus	GPa
E_{hkl}	Elastic modulus of the diffraction plane	GPa
G_x	Total intensity diffracted by a finite layer expressed as a fraction of the total diffracted intensity (see Ref. 2)	
{hkl}	Miller indices describing a family of crystalline planes	
I_0	Beam intensity	
L	Distance from the point of diffraction to a screen or detector	m
LPA	Lorentz-Polarization-Absorption factor	
n	An integer	
$S_{1\{hkl\}}$, $\frac{1}{2}S_{2\{hkl\}}$	X-ray elastic constants of the family of planes {hkl}	MPa^{-1}
χ (chi)	Angle of rotation in the plane normal to that containing omega and 2-theta about the axis of the incident beam.	°
$2\theta_{\phi\psi}$	Peak position in the direction of the measurement	°
ϕ (phi)	Angle between a fixed direction in the plane of the sample and the projection in that plane of the normal of the diffracting plane	°
ψ (psi)	Angle between the normal of the sample and the normal of the diffracting plane (bisecting the incident and diffracted beams)	°
$\varepsilon_{\phi\psi}$	Strain measured in the direction of measurement defined by the angles phi, psi	
ε_1, ε_2, ε_3	Principal strains acting in the principal directions	
ε_x	Strain measured in the X direction	
ε_y	Strain measured in the Y direction	
ε_z	Strain measured in the Z direction	
σ	Normal stress	MPa
σ_x	Stress in the X direction	MPa
σ_1, σ_2, σ_3	Principal stresses acting in the principal directions	MPa
σ_ϕ	Single stress acting in a chosen direction i.e. at an angle ϕ to σ_1	MPa
θ	Angular position of the diffraction lines according to Bragg's Law	°
ν	Poisson's ratio	
μ	Linear absorption coefficient	
τ	Normal shear stress	MPa
λ	Wavelength of the X-ray	Å
ω (omega)	Angular rotation about a reference point -the angular motion of the goniometer of the diffraction instrument in the scattering plane	°
1, 2, 3	Principal directions relevant to Cartesian co-ordinate axis	
x, y, z	Directions relevant to Cartesian co-ordinate axis	

5 Principles

The measurement of residual stress by X-ray diffraction (XRD) relies on the fundamental interactions between the wave front of the X-ray beam, and the crystal lattice. For further information regarding these interactions the reader is referred to Huygen's principle and Young's double slit experiments[1]. The basis of all XRD measurements is described in Bragg's Law, which is discussed below.

5.1 Bragg's Law

Consider a crystalline material made up of many crystals, where a crystal can be defined as *a solid composed of atoms arranged in a pattern periodic in three dimensions*[1]. These periodic planes of atoms can cause constructive and/or destructive interference patterns by diffraction. The nature of the interference depends on the inter-planar spacing d, and the wavelength of the incident radiation λ.

In 1912 W. L. Bragg (1890-1971) analysed some results from experiments conducted by the German physicist von Laue (1879-1960), in which a crystal of copper sulphate was placed in the path of an X-ray beam. A photographic plate was arranged to record the presence of any diffracted beams and a pattern of spots was formed on the photographic plate. Bragg deduced an expression for the conditions necessary for diffraction to occur in such a constructive manner.

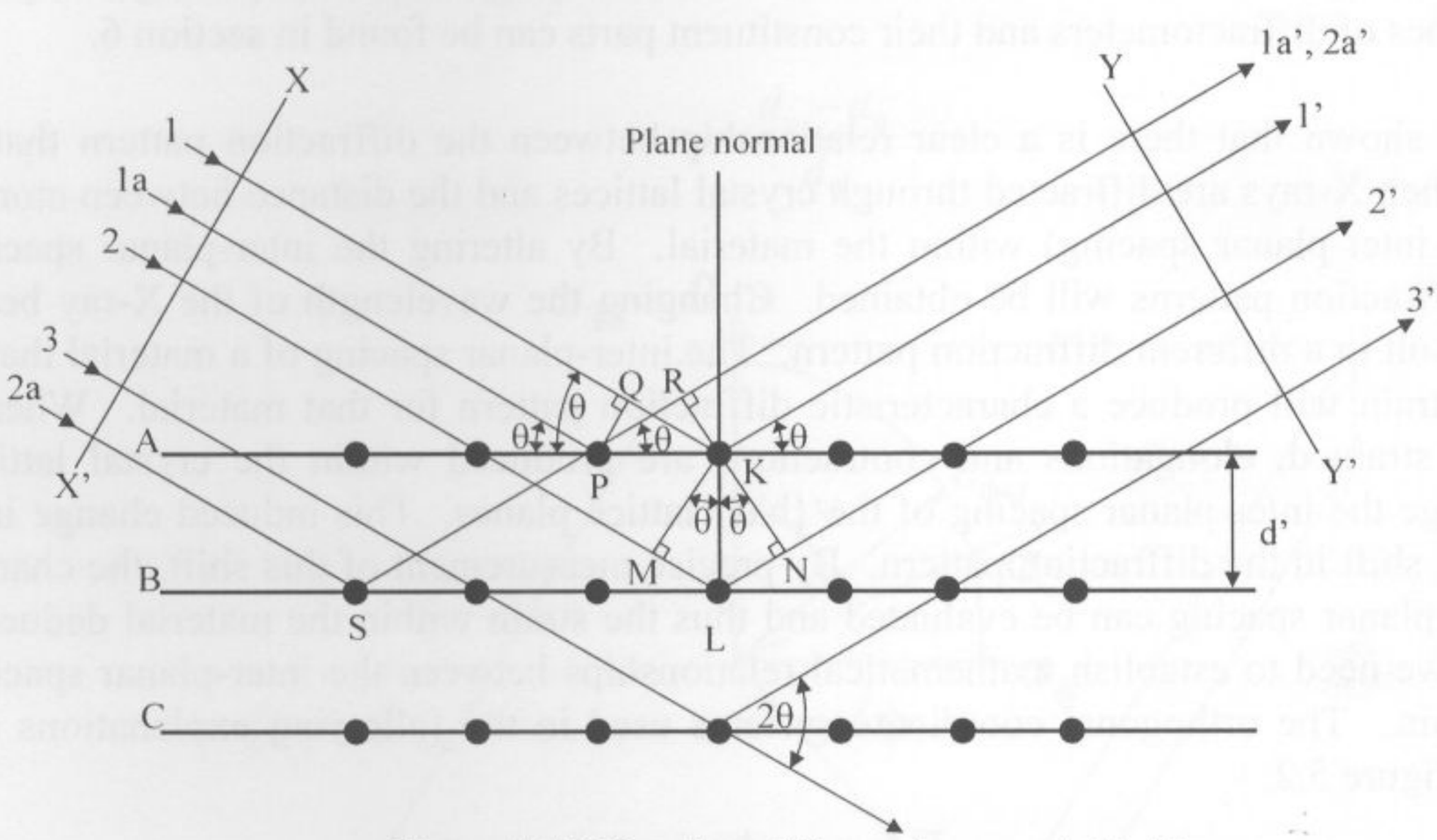

Figure 5.1 Diffraction of X-rays by a crystal lattice.

To explain Bragg's Law first consider a single plane of atoms, (row A in Figure 5.1). Ray **1** and **1a** strike atoms **K** and **P** in the first plane of atoms and are scattered in all directions. Only in directions **1'** and **1a'** are the scattered beams in phase with each other, and hence interfere constructively. Constructive interference is observed because the difference in their path length between the wave fronts XX' and YY' is equal to zero. That is

$$QK - PR = PK\cos\theta - PK\cos\theta = 0 \qquad 1$$

Any rays that are scattered by other atoms in the plane that are parallel to **1'** will also be in phase and thus add their contributions to the diffracted beam, thereby increasing the intensity. Now consider the condition necessary for constructive interference of rays scattered by atoms in different planes. Rays **1** and **2** are scattered by atoms **K** and **L**. The path difference for rays **1K1'** and **2L2'** can be expressed as

$$ML + LN = d'\sin\theta + d'\sin\theta \qquad 2$$

This term also defines the path difference for reinforcing rays scattered from atoms **S** and **P** in the direction shown in Figure 5.1, since in this direction there is no path difference between rays scattered by atoms **S** and **L** or **P** and **K**. Scattered rays **1'** and **2'** will be in phase only if the path difference is equal to a whole number n of wavelengths, that is if

$$n\lambda = 2d'\sin\theta \qquad 3$$

This is now commonly known as Bragg's Law and it forms the fundamental basis of X-ray diffraction theory.

5.2 Strain Measurement

To perform strain measurements the specimen is placed in the X-ray diffractometer, and it is exposed to an X-ray beam that interacts with the crystal lattice to cause diffraction patterns. By scanning through an arc of radius about the specimen the diffraction peaks can be located and the necessary calculations made, as detailed below. Further information regarding the different types of diffractometers and their constituent parts can be found in section 6.

It has been shown that there is a clear relationship between the diffraction pattern that is observed when X-rays are diffracted through crystal lattices and the distance between atomic planes (the inter-planar spacing) within the material. By altering the inter-planar spacing different diffraction patterns will be obtained. Changing the wavelength of the X-ray beam will also result in a different diffraction pattern. The inter-planar spacing of a material that is free from strain will produce a characteristic diffraction pattern for that material. When a material is strained, elongations and contractions are produced within the crystal lattice, which change the inter-planar spacing of the {hkl} lattice planes. This induced change in d will cause a shift in the diffraction pattern. By precise measurement of this shift, the change in the inter-planar spacing can be evaluated and thus the strain within the material deduced. To do this we need to establish mathematical relationships between the inter-planar spacing and the strain. The orthogonal coordinate systems used in the following explanations are defined in Figure 5.2.

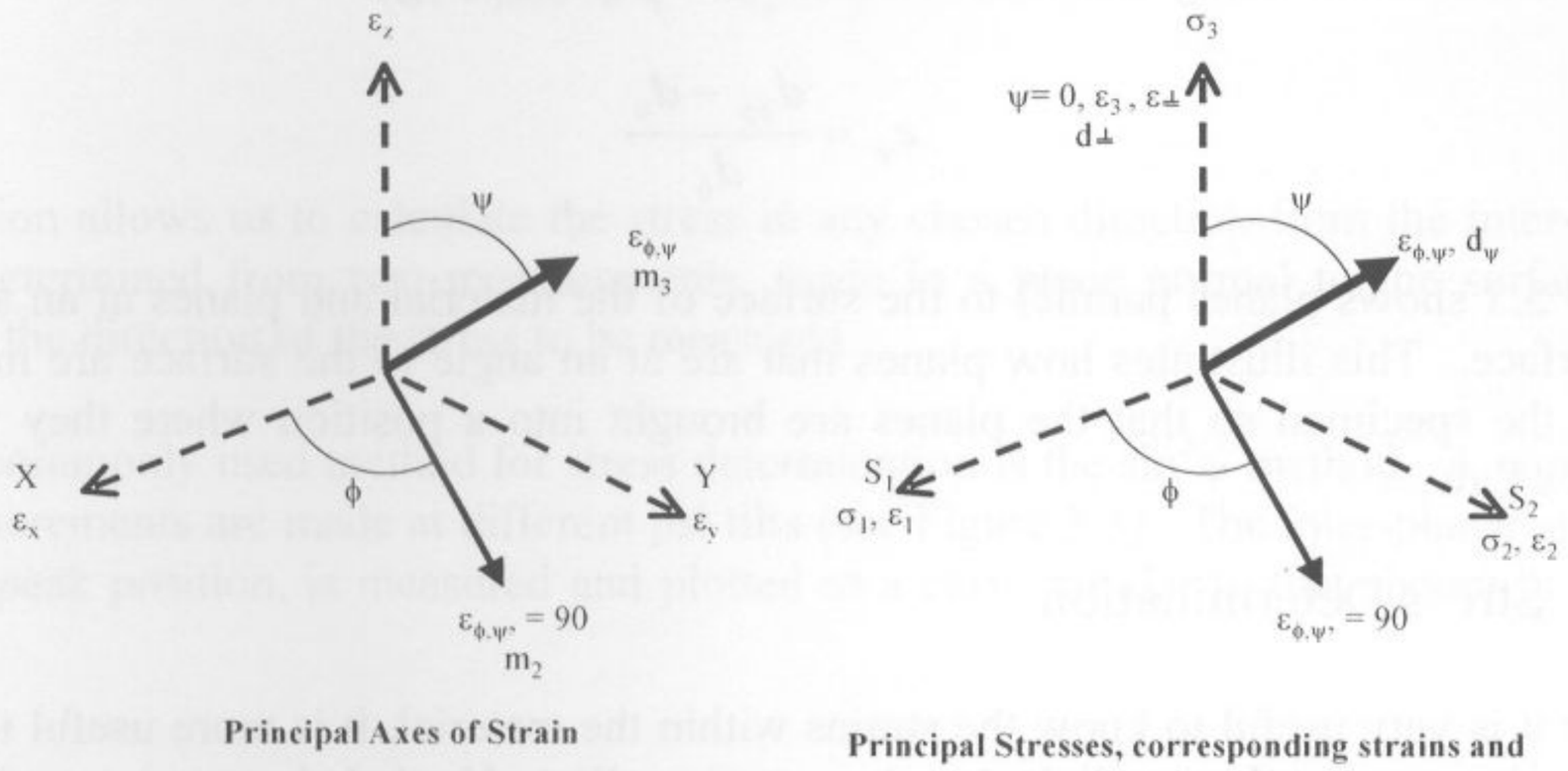

Figure 5.2 Co-ordinate system used for calculating surface strain and stresses. Note that ε_z and σ_3 are normal to the specimen surface

Let us assume that because the measurement is made within the surface, that $\sigma_3 = 0$. The strain ε_z however will not be equal to zero. The strain ε_z can be measured experimental by measuring the peak position 2θ, and solving equation 3 for a value of d_n. If we know the unstrained inter-planar spacing d_0 then;

$$\varepsilon_z = \frac{d_n - d_0}{d_0} \qquad 4$$

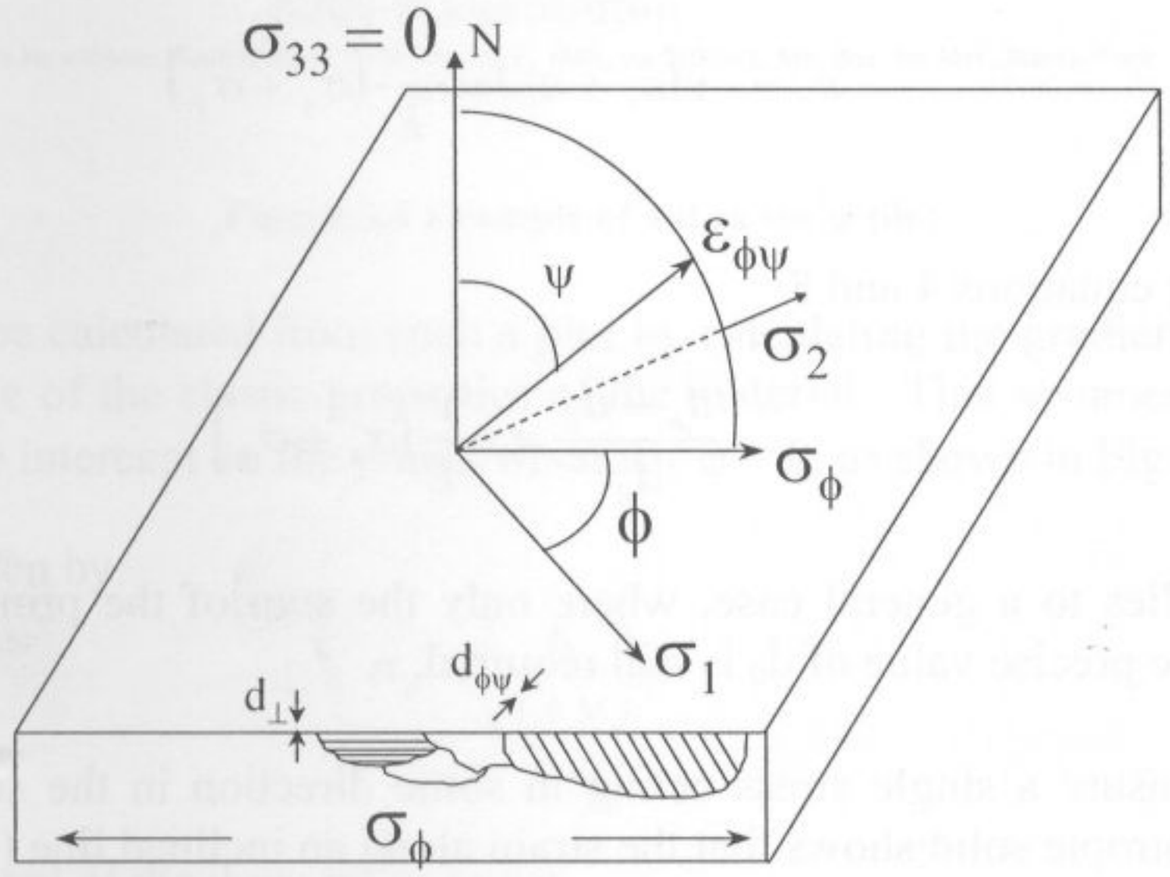

Figure 5.3 Schematic showing diffraction planes parallel to the surface and at an angle $\phi\psi$. Note σ_1 and σ_2 both lie in the plane of the specimen surface

Thus, the strain within the surface of the material can be measured by comparing the unstressed lattice inter-planar spacing with the strained inter-planar spacing. This, however, requires precise measurement of an unstrained sample of the material. Equation 4 gives the formula for measurements taken normal to the surface. By altering the tilt of the specimen

within the diffractometer, measurements of planes at an angle ψ can be made (see Figure 5.3) and thus the strains along that direction can be calculated using

$$\varepsilon_{\psi} = \frac{d_{\phi\psi} - d_0}{d_0} \qquad 5$$

Figure 5.3 shows planes parallel to the surface of the material and planes at an angle $\phi\psi$ to the surface. This illustrates how planes that are at an angle to the surface are measured by tilting the specimen so that the planes are brought into a position where they will satisfy Bragg's Law.

5.3 Stress Determination

Whilst it is very useful to know the strains within the material, it is more useful to know the engineering stresses that are linked to these strains. From Hooke's law we know that

$$\sigma_y = E\varepsilon_y \qquad 6$$

It is also well know that a tensile force producing a strain in the X-direction will produce not only a linear strain in that direction but also strains in the transverse directions. Assuming a state of plane stress exists, i.e. $\sigma_z = 0$, and that the stresses are biaxial, then the ratio of the transverse to longitudinal strains is Poisson's ratio, ν;

$$\varepsilon_x = \varepsilon_y = -\nu\varepsilon_z = \frac{-\nu\sigma_y}{E} \qquad 7$$

If we assume that at the surface of the material, where the X-ray measurement can be considered to have been made (see section 5.4 on depth penetration), that $\sigma_z = 0$ then

$$\varepsilon_z = -\nu(\varepsilon_x + \varepsilon_y) = \frac{-\nu}{E}(\sigma_x + \sigma_y) \qquad 8$$

Thus combining equations 4 and 8

$$\frac{d_n - d_0}{d_0} = -\frac{\nu}{E}(\sigma_x + \sigma_y) \qquad 9$$

Equation 9 applies to a general case, where only the sum of the principal stresses can be obtained, and the precise value of d_0 is still required.

We wish to measure a single stress acting in some direction in the surface σ_ϕ. Elasticity theory for an isotropic solid shows that the strain along an inclined line (m_3 in Figure 5.2) is

$$\varepsilon_{\phi\psi} = \frac{1+\nu}{E}(\sigma_1 \cos^2\phi + \sigma_2 \sin^2\phi)\sin^2\psi - \frac{\nu}{E}(\sigma_1 + \sigma_2) \qquad 10$$

If we consider the strains in terms of inter-planar spacing, and use the strains to evaluate the stresses, then it can be shown that

$$\sigma_\phi = \frac{E}{(1+\nu)\sin^2\psi}\left(\frac{d_\psi - d_n}{d_n}\right) \qquad 11$$

This equation allows us to calculate the stress in any chosen direction from the inter-planar spacings determined from two measurements, made in a plane normal to the surface and containing the direction of the stress to be measured.

The most commonly used method for stress determination is the $\sin^2\psi$ method. A number of XRD measurements are made at different psi tilts (see Figure 5.3). The inter-planar spacing, or 2-theta peak position, is measured and plotted as a curve similar to that shown in Figure 5.4.

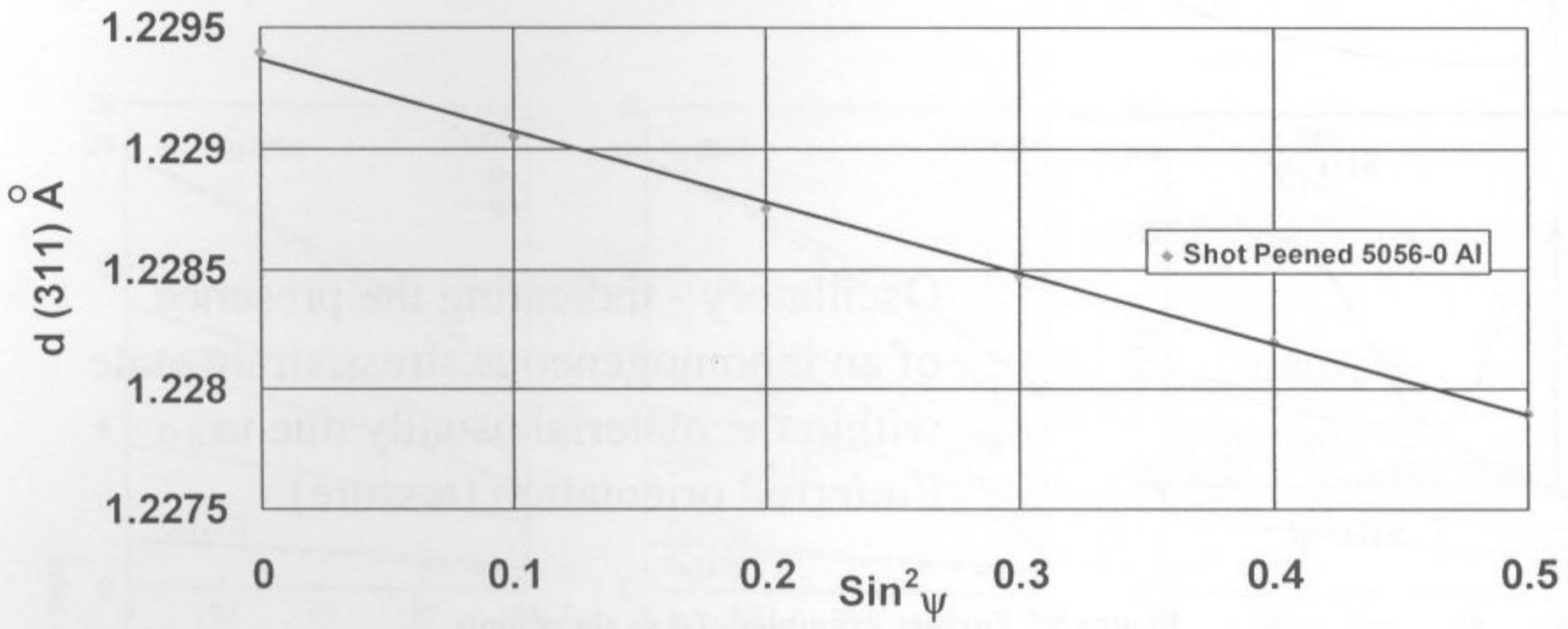

Linear dependence of d (311) upon $\sin^2\psi$ for shot peened 5056-0 aluminium

Prevey, P.S. "Metals Handbook: Ninth Edition," Vol. 10, ed. K. Mills, pp 380-392, Am. Soc. for Met., Metals Park, Ohio (1986)

Figure 5.4 Example of a d vs $\sin^2\psi$ plot

The stress can then be calculated from such a plot by calculating the gradient of the line and with basic knowledge of the elastic properties of the material. This assumes a zero stress at $d = d_n$, where d is the intercept on the y-axis when $\sin^2\psi = 0$, as shown in Figure 5.4.

Thus the stress is given by:

$$\sigma_\phi = \left(\frac{E}{1+\nu}\right)m \qquad 12$$

Where m is the gradient of the d vs. $\sin^2\psi$ curve.

For the full derivation of this solution the reader is referred to Ref. 1 and 2.

This is the basis of stress determination using X-ray diffraction. More complex solutions exist for non-ideal situations where, for example, psi splitting occurs (caused by the presence of shear stresses) or there is an inhomogeneous stress state within the material (Figure 5.5).

Such solutions are available within the literature and may be embedded within software packages.

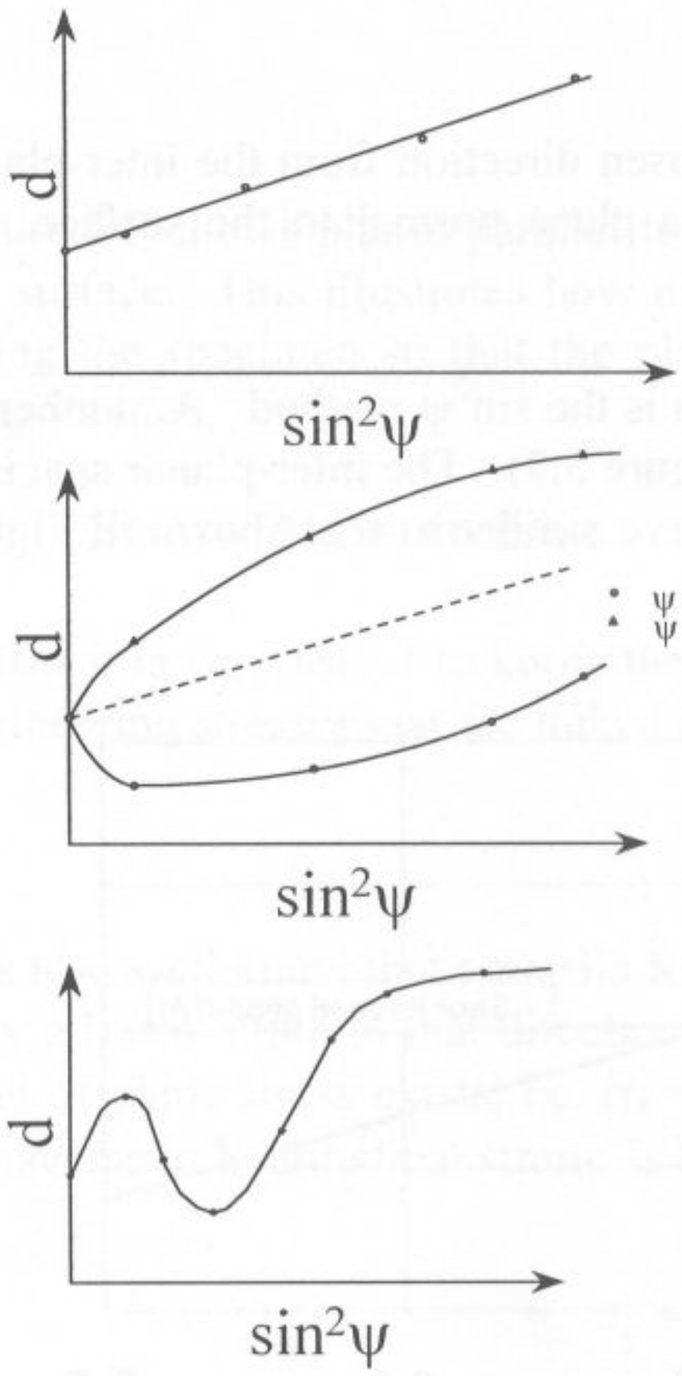

Regular d vs $\sin^2\psi$ behaviour with ε_{13} and ε_{23} being zero.

ψ-splitting - ε_{13} and/or ε_{23} are non-zero.

Oscillatory - indicating the presence of an inhomogeneous stress/strain state within the material usually due to Preferred orientation (texture).

Figure 5.5 Further examples of d vs $\sin^2\psi$ plots

Equation 11 assumes that the bulk modulus is the same as the modulus of the lattice plane being used for the measurement; this assumption is often not the case. A better method is to calculate or measure the elastic constants of a particular plane. To measure these constants a bending test must be performed in the diffractometer, and the reader is referred to ASTM E-1426-94 for further information. Most modern software will calculate the plane-specific constants for the analysis routines, but this may not be the case for all.

5.4 Depth of Penetration

Many metallic specimens strongly absorb X-rays, and because of this the intensity of the incident beam is greatly reduced in a very short distance below the surface. Consequently the majority of the diffracted beam originates from a thin surface layer, and hence the residual stress measurements correspond only to that layer of the material. This begs the question of what is the effective penetration depth of X-rays and to what depth in the material does the diffraction data truly apply? This is not a straightforward question to answer and is dependent on many factors that include the absorption coefficient of the material for a particular beam, and the beam dimensions on the specimen surface.

No precise answer can be given for the penetration depth. What is observed is that the intensity decreases exponentially with depth in the material. The rationale for this is as follows: the attenuation, loss in signal strength, is proportional to the distance travelled in a material, hence the contribution to the diffracted beam from layers, or planes, deeper down in

the material becomes less. Coupled with this is the fact that the diffracted beam still has to exit the material, thereby travelling through more material and suffering more attenuation.

The thickness (x) of the effective layer can be calculated, and is shown below in equation 13. The full derivation is presented in Ref. 2.

$$x = \frac{\ln\left[\dfrac{1}{1-G_x}\right]}{\mu\left[\dfrac{1}{\sin(\theta+\psi)} + \dfrac{1}{\sin(\theta-\psi)}\right]} \qquad 13$$

Figures 5.6 shows the penetration depths vs. sin2ψ for materials commonly used for residual stress measurements. The difference in the effective layer thickness with ψ angles becomes of greater importance when the test specimen exhibits a steep stress gradient [3].

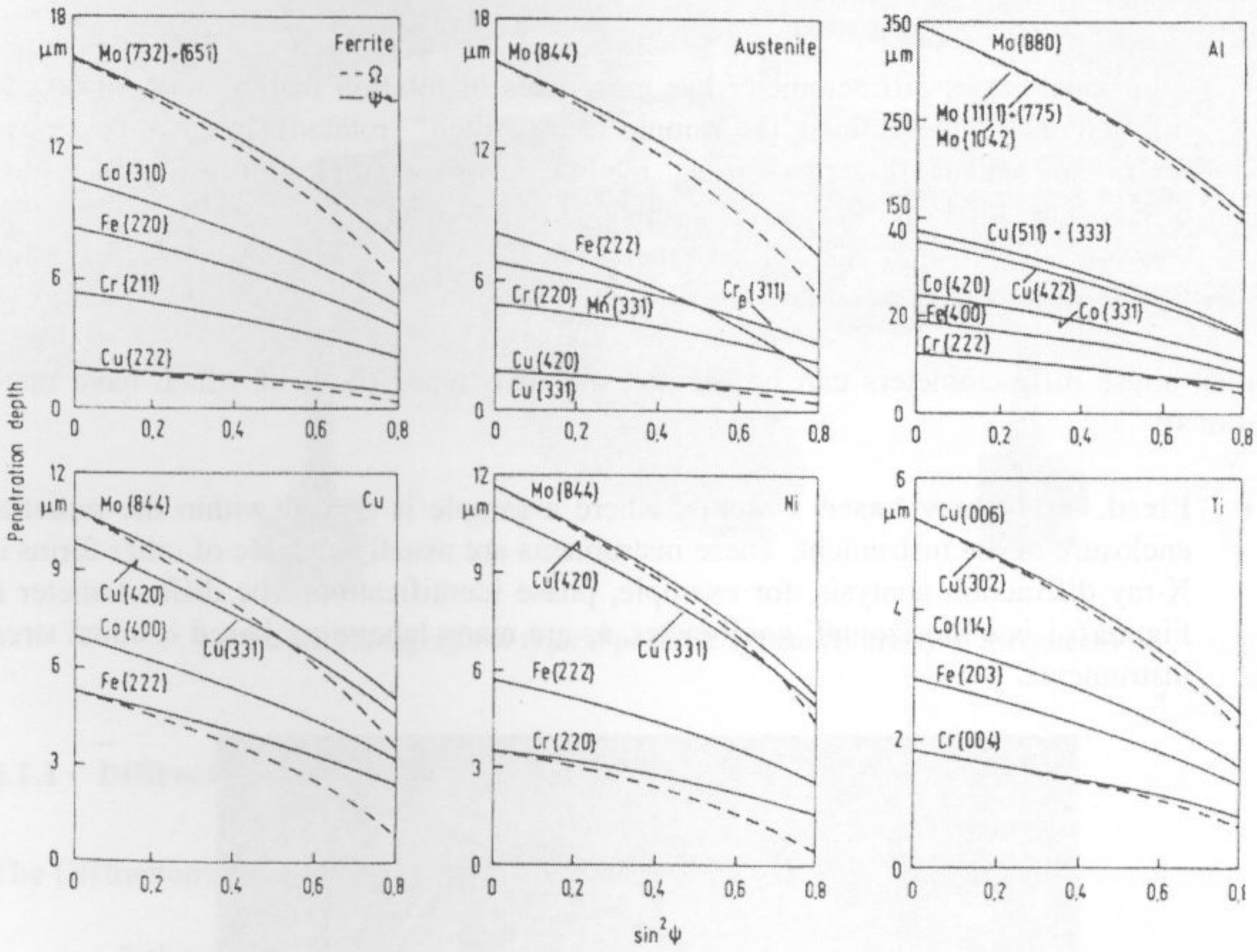

Figure 5.6 Penetration depths vs. $\sin^2\psi$ of different metals and radiations (After Ref. 5)

6 Apparatus

6.1 General

The diffractometers used for the measurement of residual stress are basically powder diffractometers, however they differ in the following ways:

- They can accommodate larger, heavier samples, as it is not usually desirable to cut small sections from large components.

- The maximum 2θ angle accessible to the instrument is large, typically 165° 2θ. (Most powder diffractometers cannot exceed 145° 2θ). Measurements can be made at very high 2θ values where the small changes in the d-spacings, due to strain, can be measured more precisely.

- A residual stress diffractometer has more axes of rotation than a standard powder diffractometer. This allows the sample to be "tilted" (rotated), in accordance with the requirements of the $\sin^2\psi$ method. For example, in residual stress diffractometers, both omega and 2-theta can be moved independently, i.e. they are "de-coupled". In a powder diffractometer omega is often fixed, mechanically, at half the value of 2-theta.

Residual stress diffractometers can be divided into two types (both of which have many variations):

- **Fixed, laboratory based systems,** where a sample is placed within the radiation enclosure of the instrument. These instruments are usually capable of other forms of X-ray diffraction analysis, for example, phase identification. The diffractometer in Figure 6.1 is a 'horizontal' goniometer, as are many laboratory based residual stress instruments.

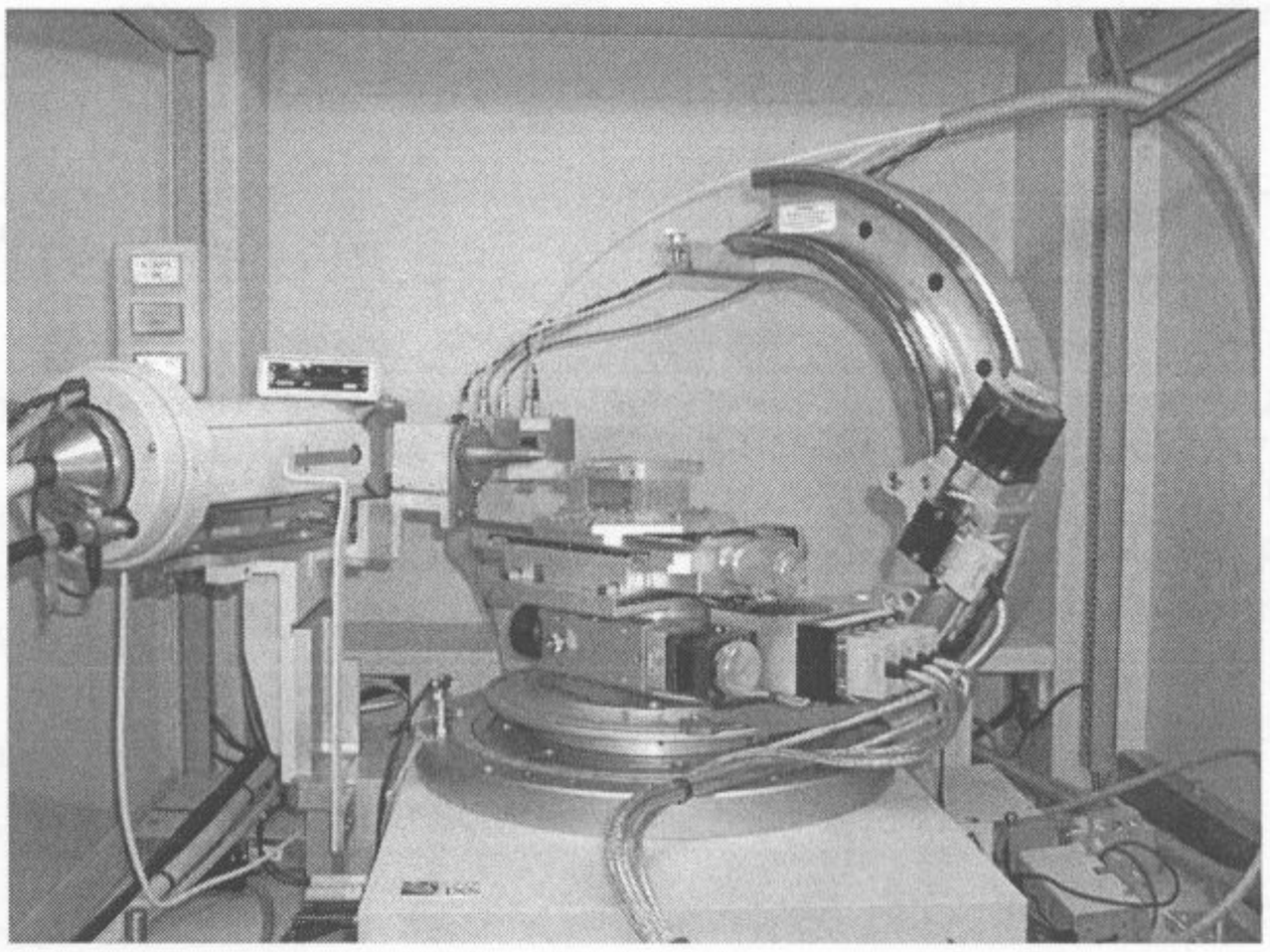

Figure 6.1 Photograph of a typical laboratory system (courtesy of The Open University)

- **Portable systems**. These are designed specifically for stress analysis and are much smaller; they can often be carried easily. They can be taken to a large structure (for example, a bridge) and placed on the component of interest. Generally, they are much simpler in construction than laboratory based systems. They are designed to access small areas and awkward shaped components, such as gear teeth. (Figure 6.2)

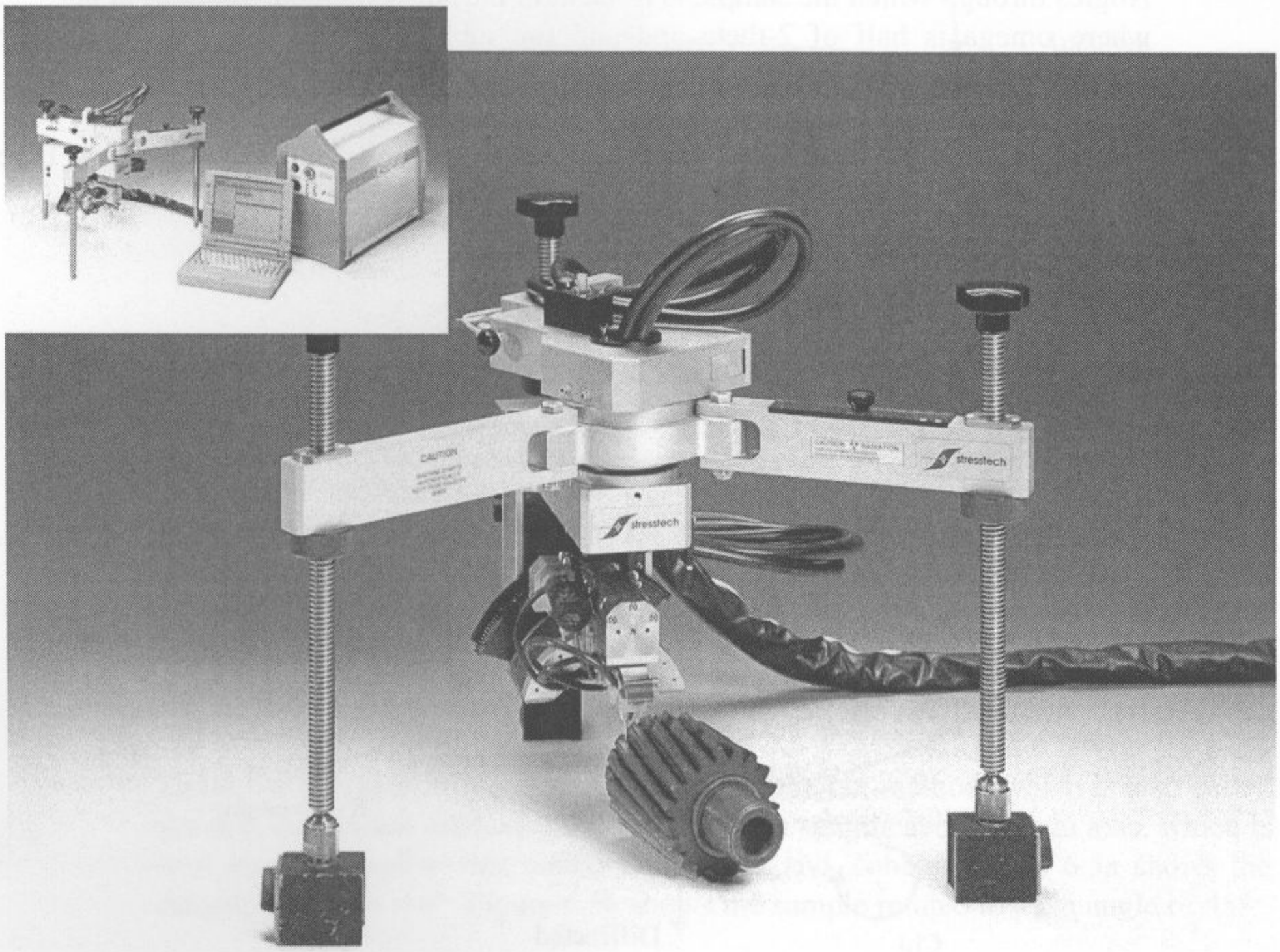

Figure 6.2 Photograph of typical portable system (courtesy of Stresstech)

6.1.1 Diffraction Geometry

The Diffractometer angles used in residual stress analysis are:

- **2-theta (2θ)**
  The Bragg angle, this is the angle between the incident (transmitted) and diffracted X-ray beams.

- **Omega (ω)**
  The angle between the incident X-ray beam and the sample surface.
  Both omega and 2-theta lie in the same plane.

- **Phi (ϕ)**
  The angle of rotation of the sample about its surface normal.

- **Chi (χ)**
  Chi rotates in the plane normal to that containing omega and 2-theta. This angle is also sometimes (confusingly) referred to as ψ.

- **Psi (ψ)**
  Angles through which the sample is rotated, in the $\sin^2\psi$ method. We start at psi = 0, where omega is half of 2-theta and add (or subtract) successive psi offsets, for example, 10, 20, 30 and 40°.

These angles are illustrated in Figure 6.3, which shows the arrangement in a laboratory type goniometer measuring a large 2-theta angle, as used in residual stress analysis.

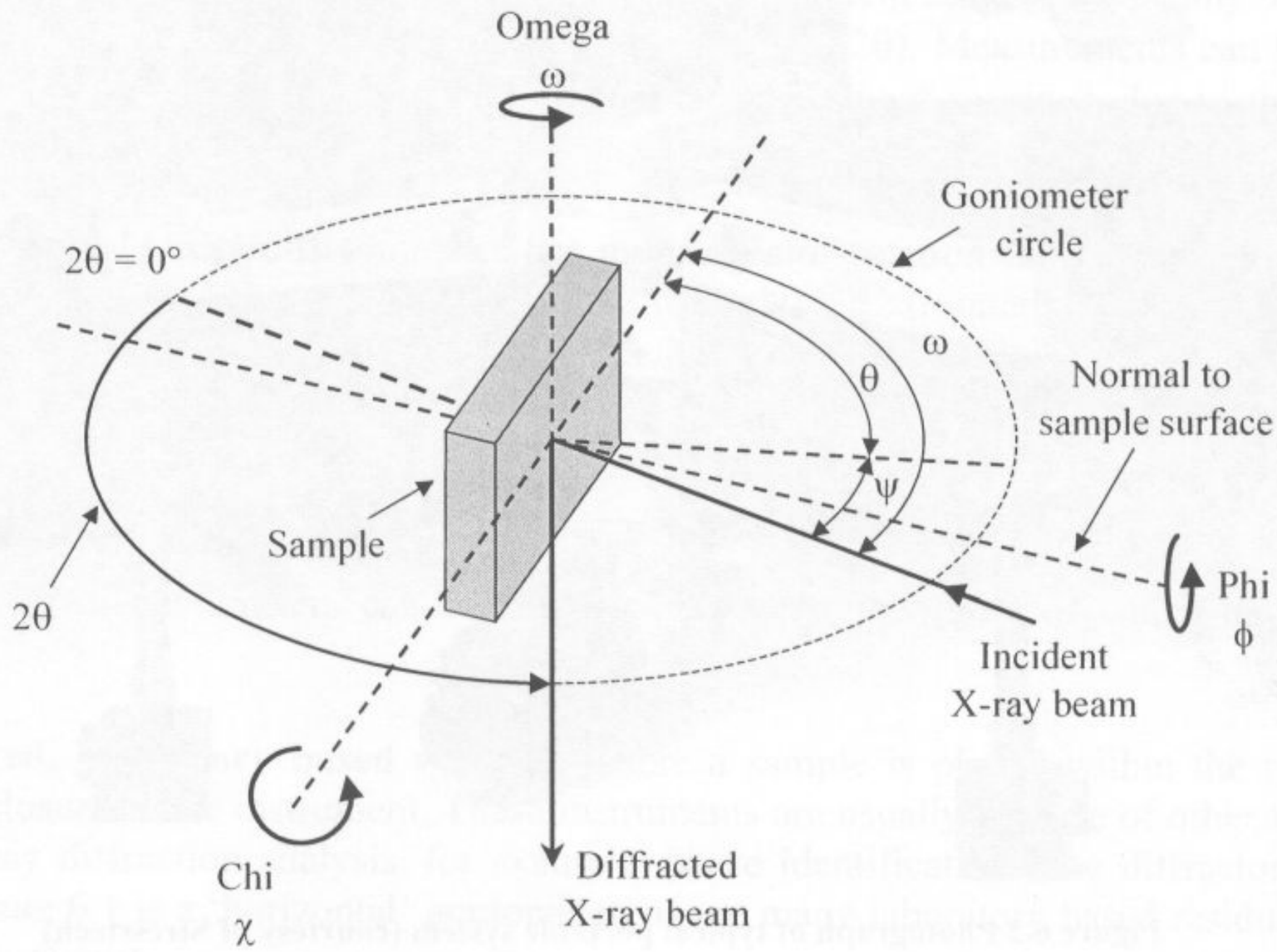

Figure 6.3 Angles and rotations used in residual stress measurement (For a horizontal system with a positive psi offset.)

There are two methods of rotating the sample when residual stress is measured by the $\sin^2\psi$ technique:

- **The Omega Method**
  Here we rotate (tilt) the sample about the omega axis. Both omega and 2-theta are in the same plane. The values of psi are added, for positive psi (or subtracted, for negative psi), to theta. Most conventional powder diffractometers, with a de-coupled omega drive (where the omega and 2-theta axes are able to move independently) can make measurements using this method. The geometry is shown schematically in Figure 6.4. Omega is shown as equal to half 2-theta, i.e. in focused geometry (see Section 6.2.2 and Figures 6.10 and 6.11).

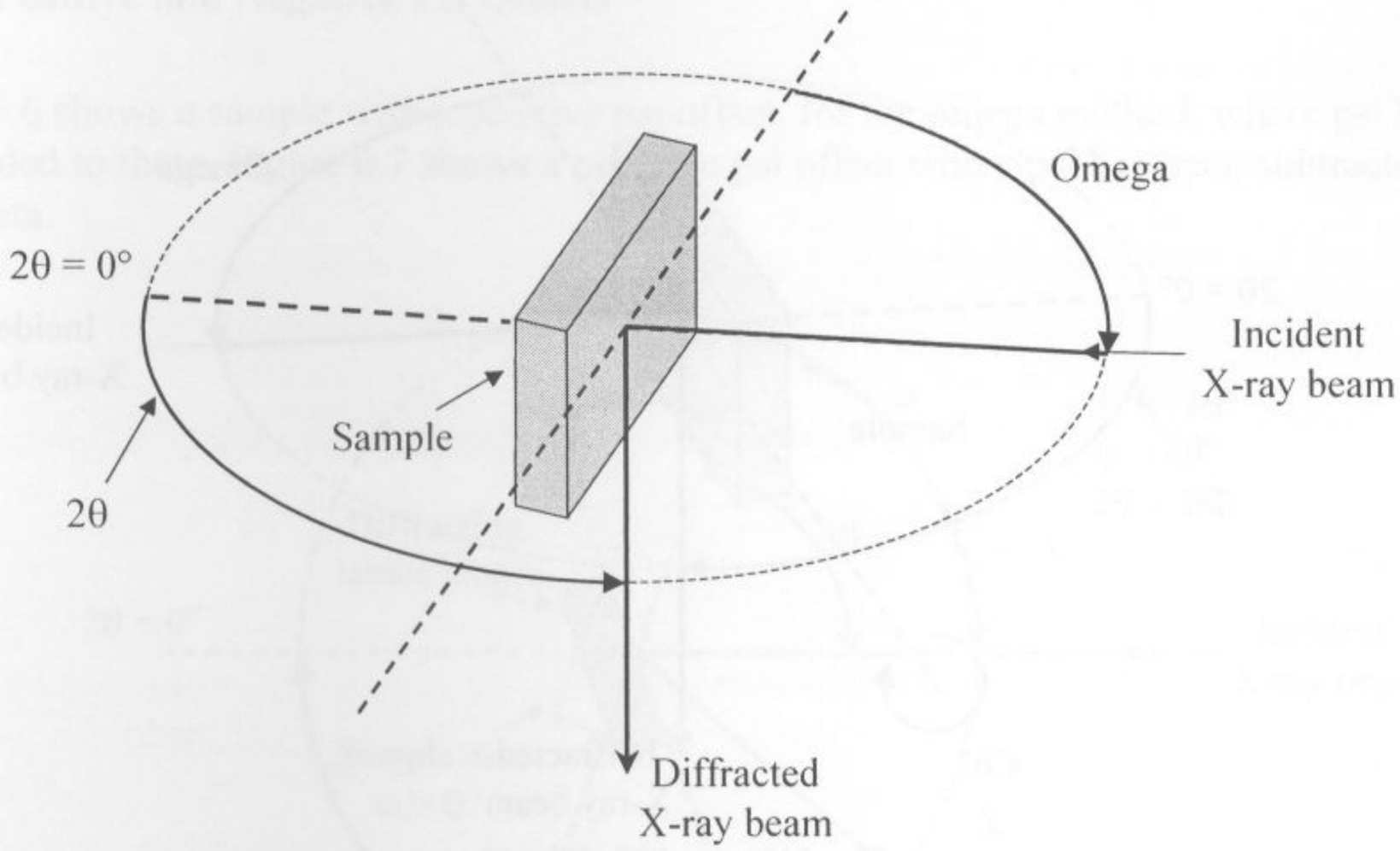

Both Omega and 2θ rotate in the same plane
(shown with Omega = 70°, 2θ = 140°, Chi = 0°)

Figure 6.4 The omega method (Horizontal laboratory-type system shown from above)

- **The Chi Method**

  Figures 6.5a and 6.5b show the geometry of the chi method, which is also called the side inclination method. Here we rotate the sample about the chi axis, which is in a plane normal to that containing omega and 2-theta. Figure 6.5a shows the sample when chi = 0°. Figure 6.5b shows the sample rotated to a chi angle of 45°.

  Mechanically the chi method is a more complex method. Laboratory based diffractometers which use the chi method incorporate a special sample stage called an Eulerian (see Figure 6.1) cradle which enables the chi and phi rotations.

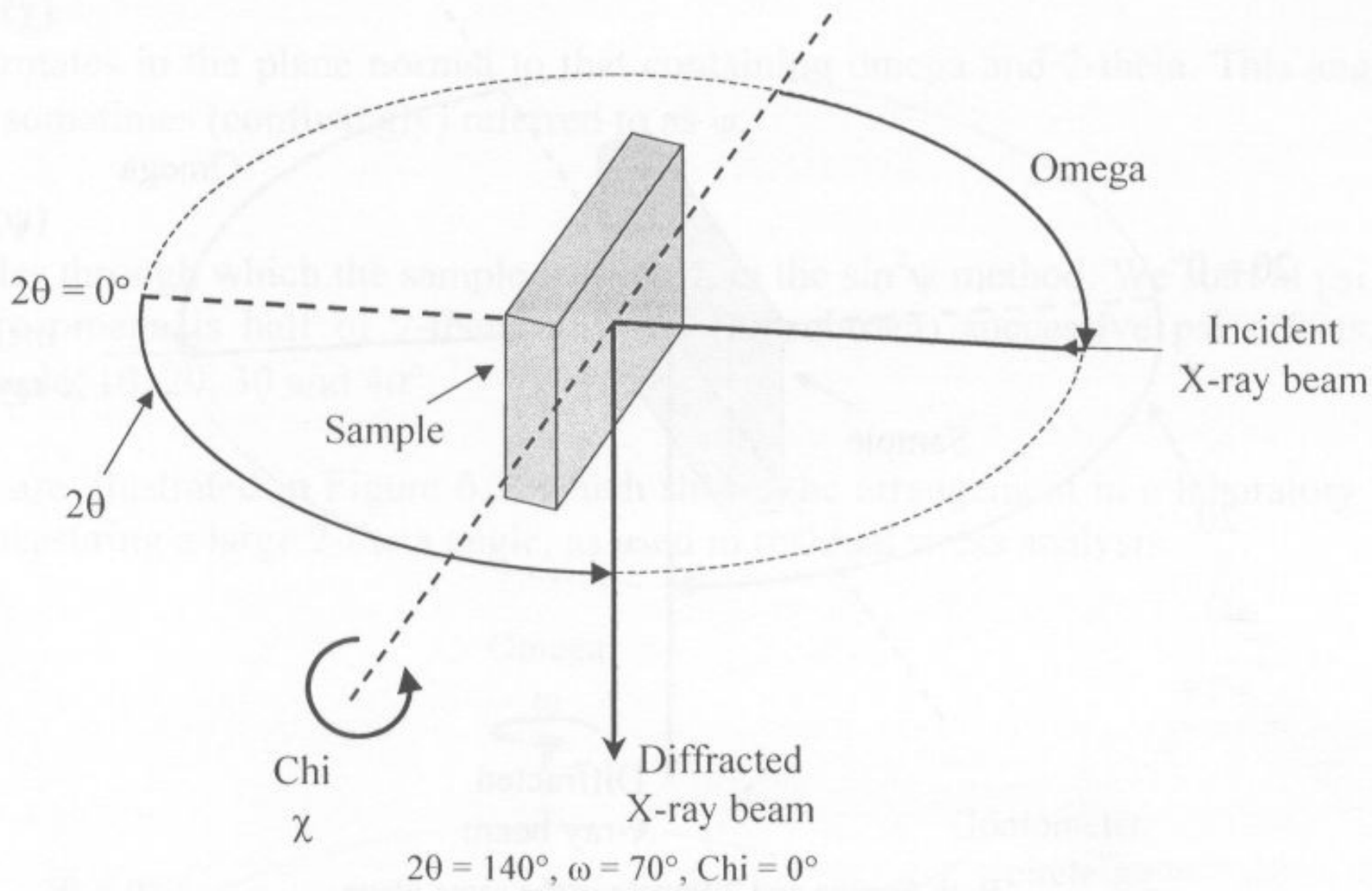

Figure 6.5a The chi method (Horizontal laboratory-type system shown from above)

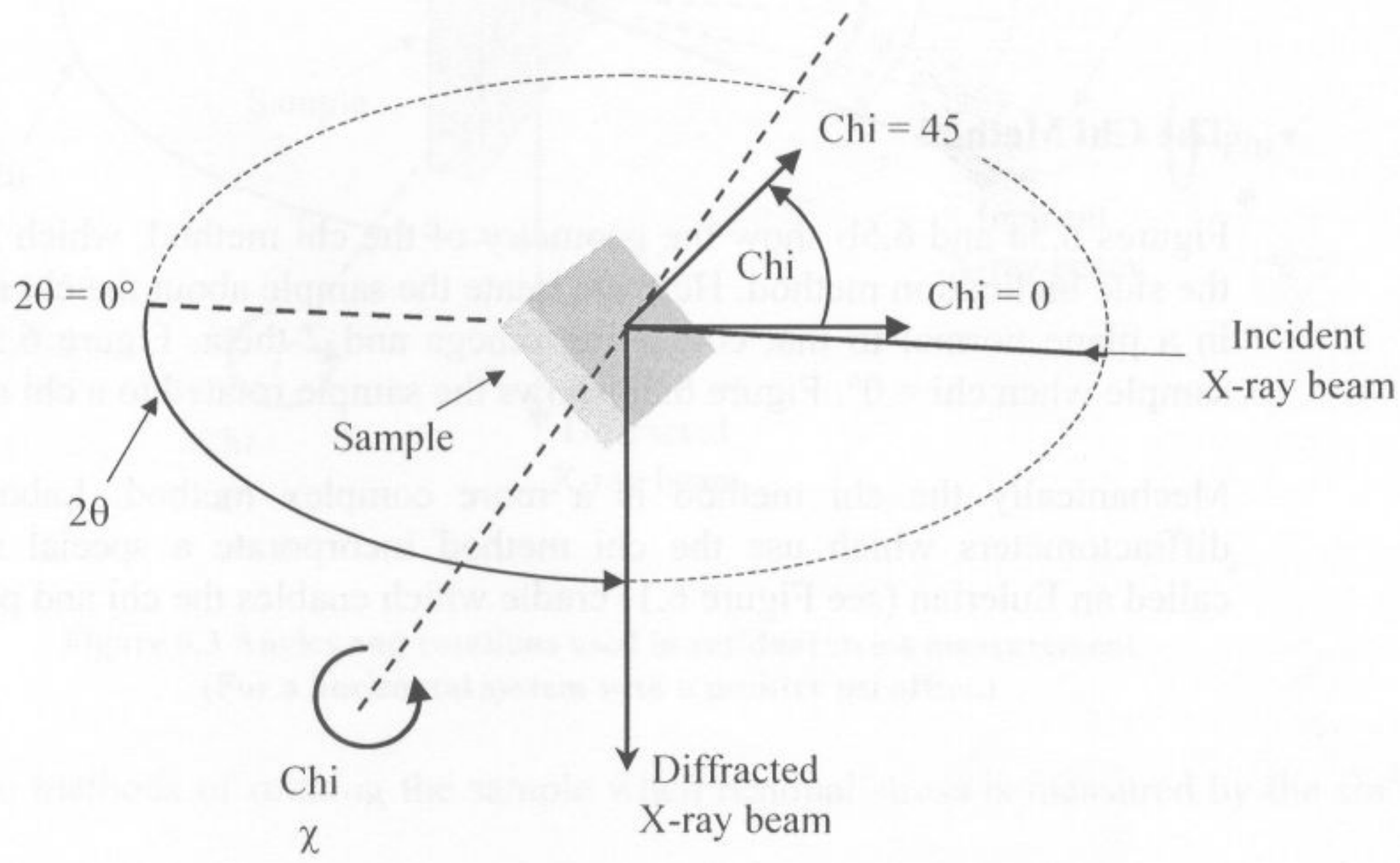

The normal to the sample surface is shown at Chi = 0° and Chi = 45°
(shown with 2θ = 140°, omega = 70° and Chi = 45°)

Figure 6.5b The chi method (Horizontal laboratory-type system shown from above)

6.1.2 Positive and Negative Psi Offsets

Figure 6.6 shows a sample with a positive psi offset, for the omega method, where psi has been added to theta. Figure 6.7 shows a negative psi offset where psi has been subtracted from theta.

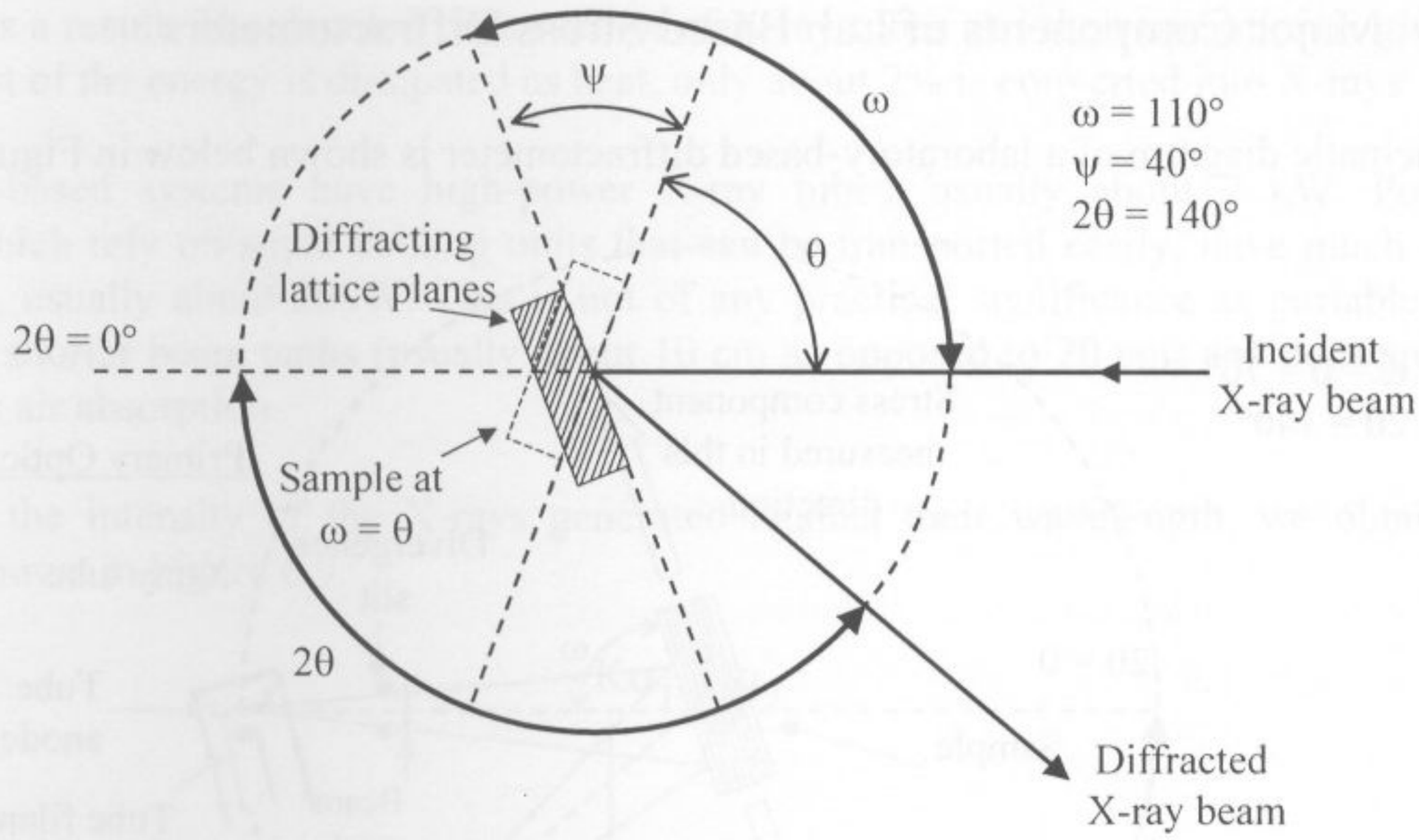

Figure 6.6 Positive psi offset ($\omega = \theta + \Psi$)

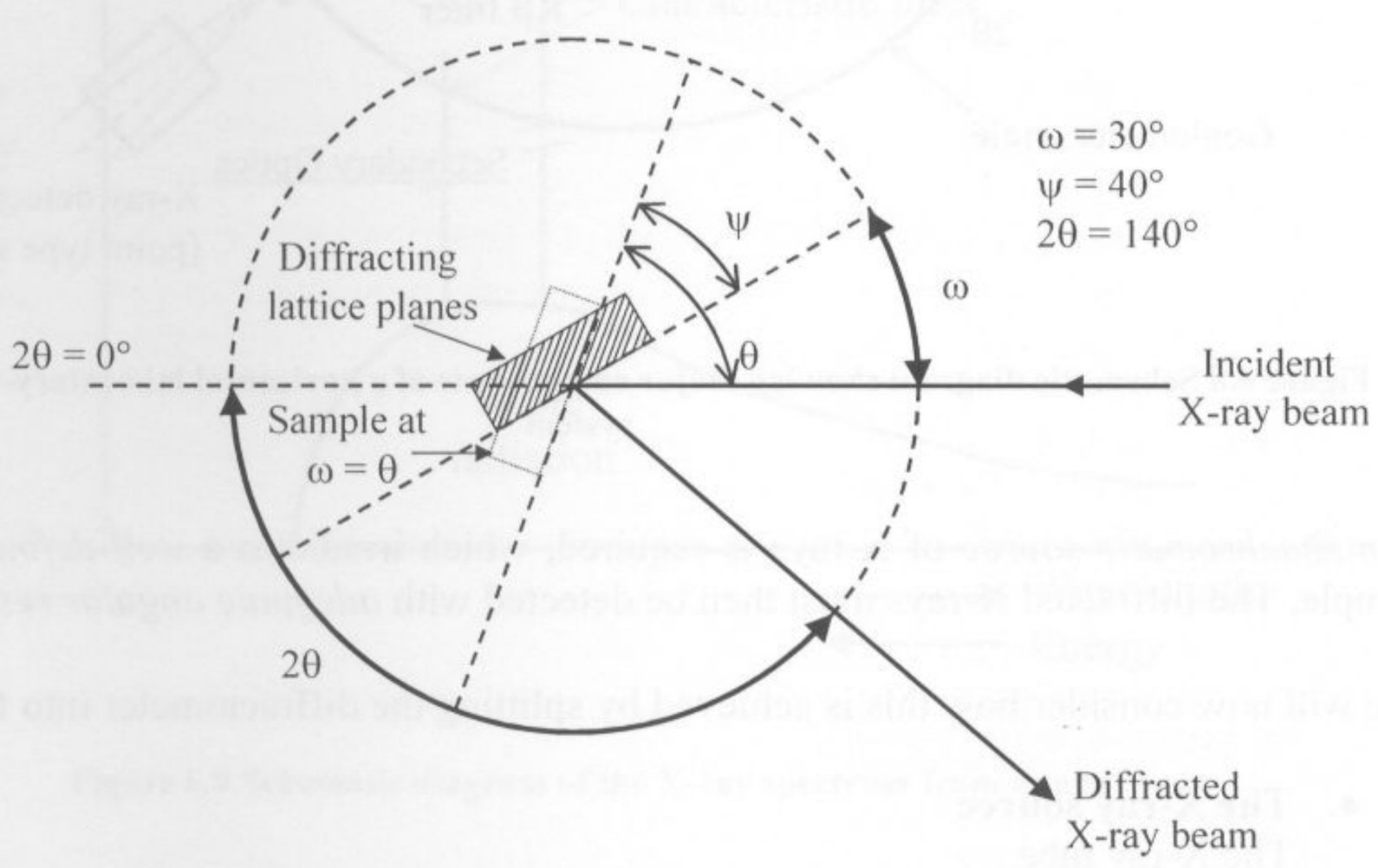

Figure 6.7 Negative psi offset ($\omega = \theta - \Psi$)

Note the small angle of incidence of the X-ray beam to the sample surface with the negative psi offset. Added to "defocusing" effects, which are discussed later, this makes the intensities from negative psi offsets lower than those from positive psi when the omega method is used. Negative psi offsets are used in the measurement of shear stresses. To avoid making measurements in negative psi, when using the omega method, we can rotate the sample

(around the phi axis) by 180° and measure positive psi. This is equivalent to a negative psi measurement without a phi rotation.

Obviously, defocusing effects are the same for positive and negative psi using the chi method, which is one of its advantages.

6.2 Major Components of Lab Based Stress Diffractometers

A schematic diagram of a laboratory-based diffractometer is shown below in Figure 6.8.

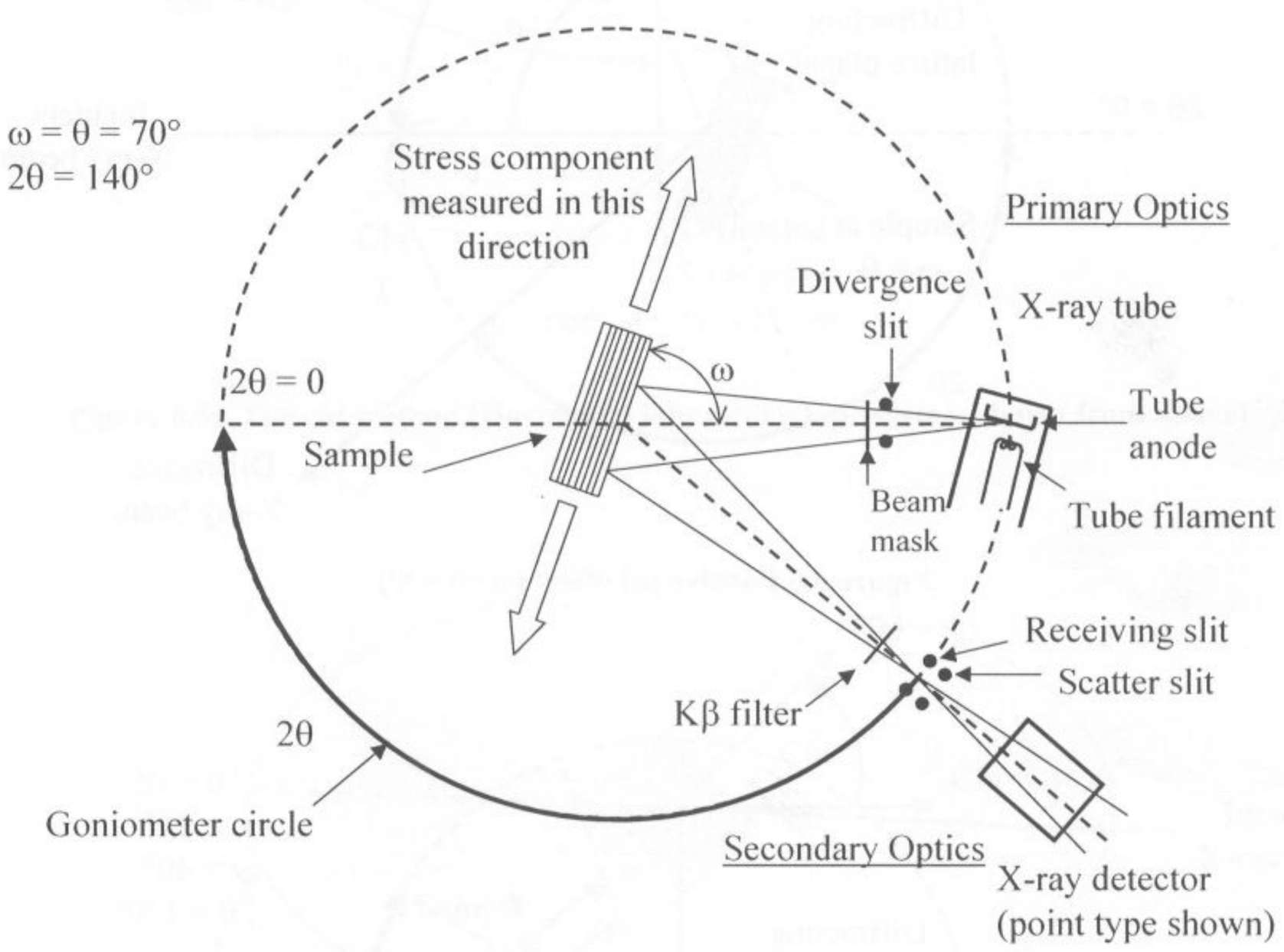

Figure 6.8 Schematic diagram showing major components of a horizontal laboratory-type focusing system

A *monochromatic source* of X-rays is required, which irradiates a *well-defined area* on the sample. The diffracted X-rays must then be detected with *adequate angular resolution.*

We will now consider how this is achieved by splitting the diffractometer into **three parts.**

- **The X-ray source**
  The X-ray tube.

- **The Primary Optics**
  These are the components between the X-ray source and the sample.

- **The Secondary Optics**
  These are the components between the sample and the detector.

6.2.1 The X-Ray Tube

All X-ray tubes work on the same principle. A focused beam of electrons is accelerated through a large potential difference (typically between 20 and 50 kV, supplied by a constant potential generator) and strikes a metal target or anode with considerable energy. X-rays are generated as a result. The detailed construction of X-ray tubes and their operation is given in Ref. 4. Most of the energy is dissipated as heat, only about 2% is converted into X-rays.

Laboratory-based systems have high-power X-ray tubes, usually about 2 kW. Portable systems, which rely on small cooling units that can be transported easily, have much lower rated tubes, usually about 200W. This is not of any practical significance as portable units have much shorter beam paths (usually about 10 cm as opposed to 20 cm) and consequently there is less air absorption.

If we plot the intensity of the X-rays generated against their wavelength, we obtain the spectrum shown in Figure 6.9.

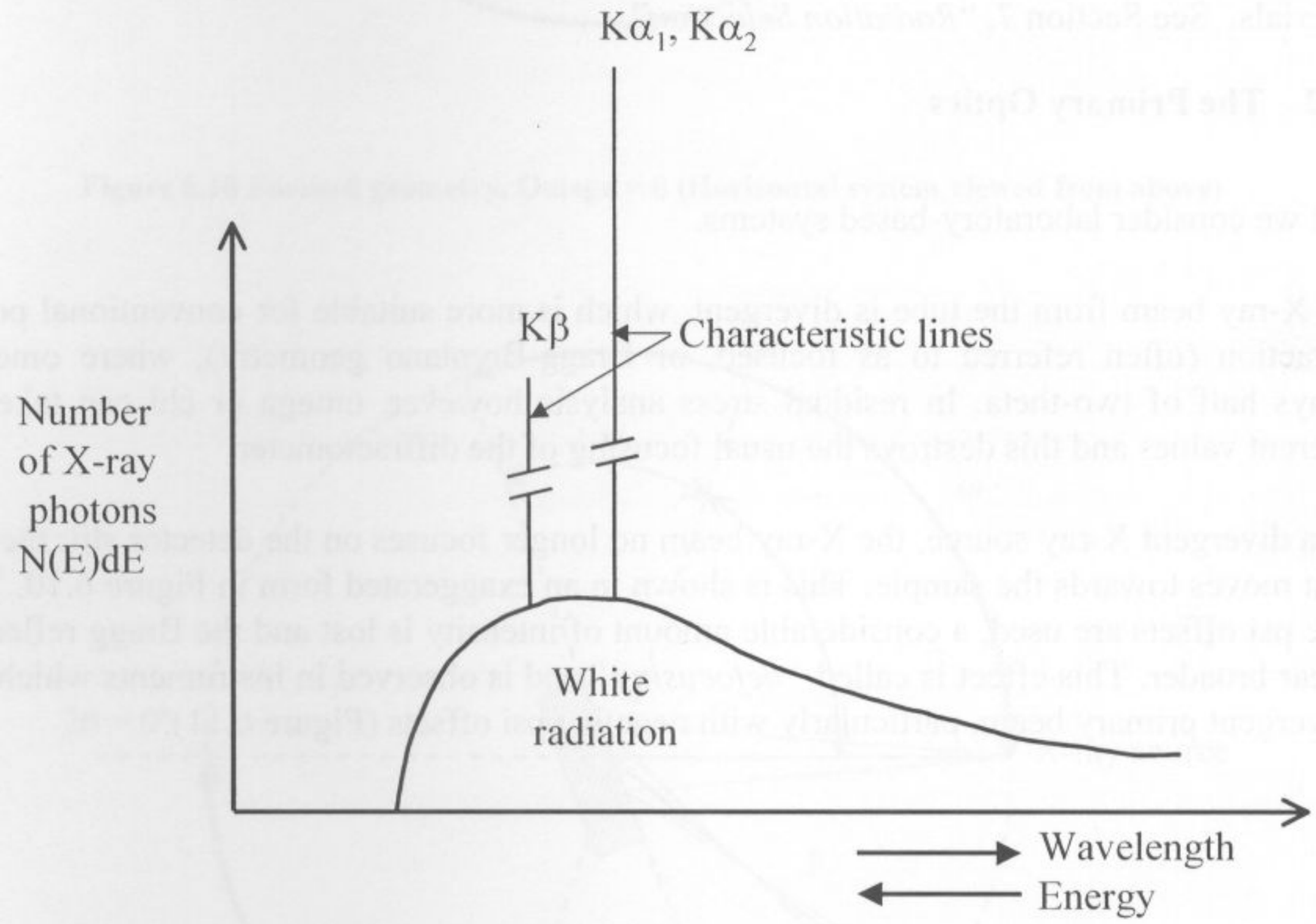

Figure 6.9 Schematic diagram of the X-ray spectrum from a tube

This X-ray spectrum can be divided into two parts:

6.2.1.1 Continuous Radiation

The smooth part of the curve is "continuous or white radiation," so-called as it is made up of many wavelengths, like white light, and is caused by the deceleration of the electrons inside the anode of the X-ray tube. As the continuous radiation is not monochromatic, it is undesirable. There are a variety of methods for reducing or removing it. The amount of

continuous radiation increases with the voltage applied to the X-ray tube and with the atomic number of the target.

6.2.1.2 Characteristic Radiation

Superimposed on the white radiation are a series of sharp, intense lines, called the characteristic lines. These have specific wavelengths and are observed when the accelerating voltage exceeds a critical value. The wavelength of the characteristic lines depends on the anode material, not on the accelerating voltage. For example, the wavelength of chromium K-α_1 is 2.290 Å and for iron K-α_1 it is 1.936 Å.

In X-ray diffraction, the K-α lines are used, as they are the most intense. The X-ray tube produces other characteristic lines, for example the K-β, which must be removed to achieve the goal of monochromatic radiation.

An X-ray tube should be selected with an anode material, which gives a suitable Bragg reflection (from our sample) at a sufficiently high 2-theta angle (ideally greater than 130° 2θ) to enable precise measurement of the *d*-spacing. Consequently, residual stress diffractometers usually have a selection of X-ray tubes available if they are to measure a wide range of materials. See Section 7, "*Radiation Selection*".

6.2.2 The Primary Optics

First we consider laboratory-based systems.

The X-ray beam from the tube is divergent, which is more suitable for conventional powder diffraction (often referred to as focused, or Bragg-Brentano geometry), where omega is always half of two-theta. In residual stress analysis however, omega or chi can take very different values and this destroys the usual focusing of the diffractometer.

For a divergent X-ray source, the X-ray beam no longer focuses on the detector slit; the focal point moves towards the sample. This is shown in an exaggerated form in Figure 6.10. When large psi offsets are used, a considerable amount of intensity is lost and the Bragg reflections appear broader. This effect is called *"defocusing"* and is observed in instruments which have a divergent primary beam, particularly with negative psi offsets (Figure 6.11).

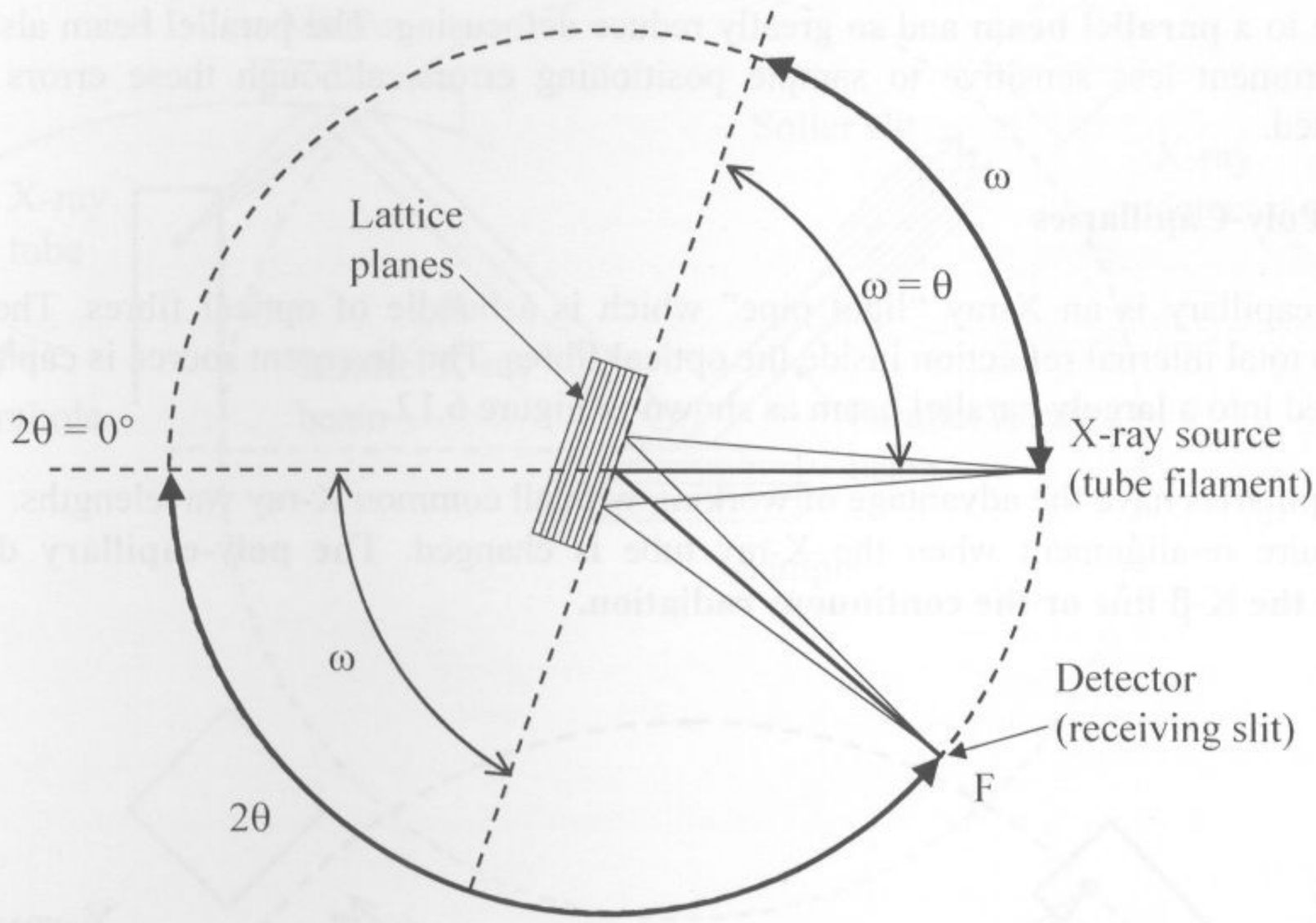

Figure 6.10 Focused geometry, Omega = θ (Horizontal system viewed from above)

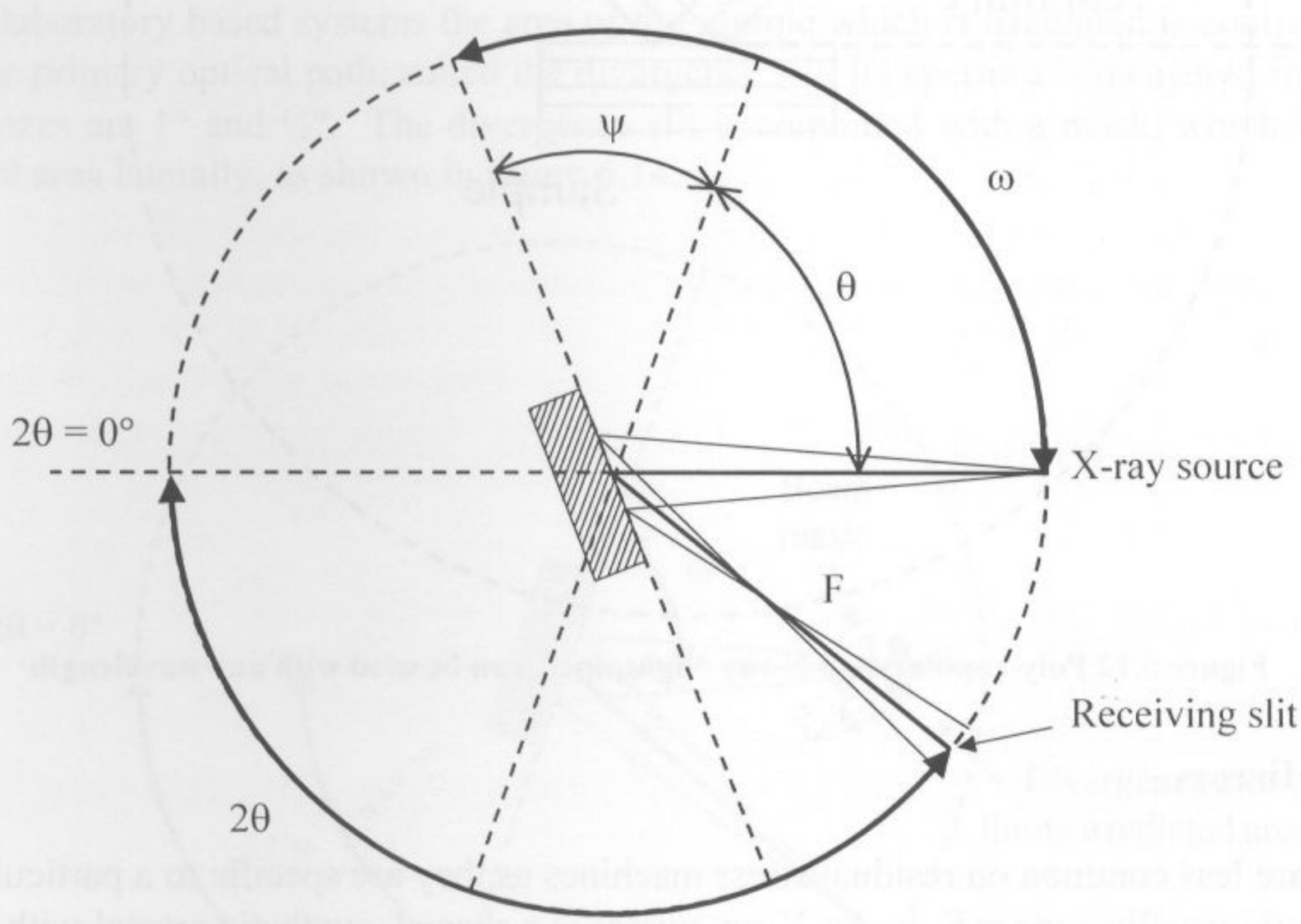

Figure 6.11 Defocused geometry, Omega = θ +Ψ (Horizontal system viewed from above)

Some residual stress diffractometers have devices to convert the divergent beam from the X-ray tube to a **parallel beam** and so greatly reduce defocusing. The parallel beam also makes the instrument less sensitive to sample positioning errors, although these errors are not eliminated.

6.2.2.1 Poly-Capillaries

A poly-capillary is an X-ray "light pipe" which is a bundle of optical fibres. The X-rays undergo total internal reflection inside the optical fibres. The divergent source is captured and converted into a largely parallel beam as shown in Figure 6.12.

Poly-capillaries have the advantage of working with all common X-ray wavelengths. They do not require re-alignment when the X-ray tube is changed. **The poly-capillary does not remove the K-β line or the continuous radiation.**

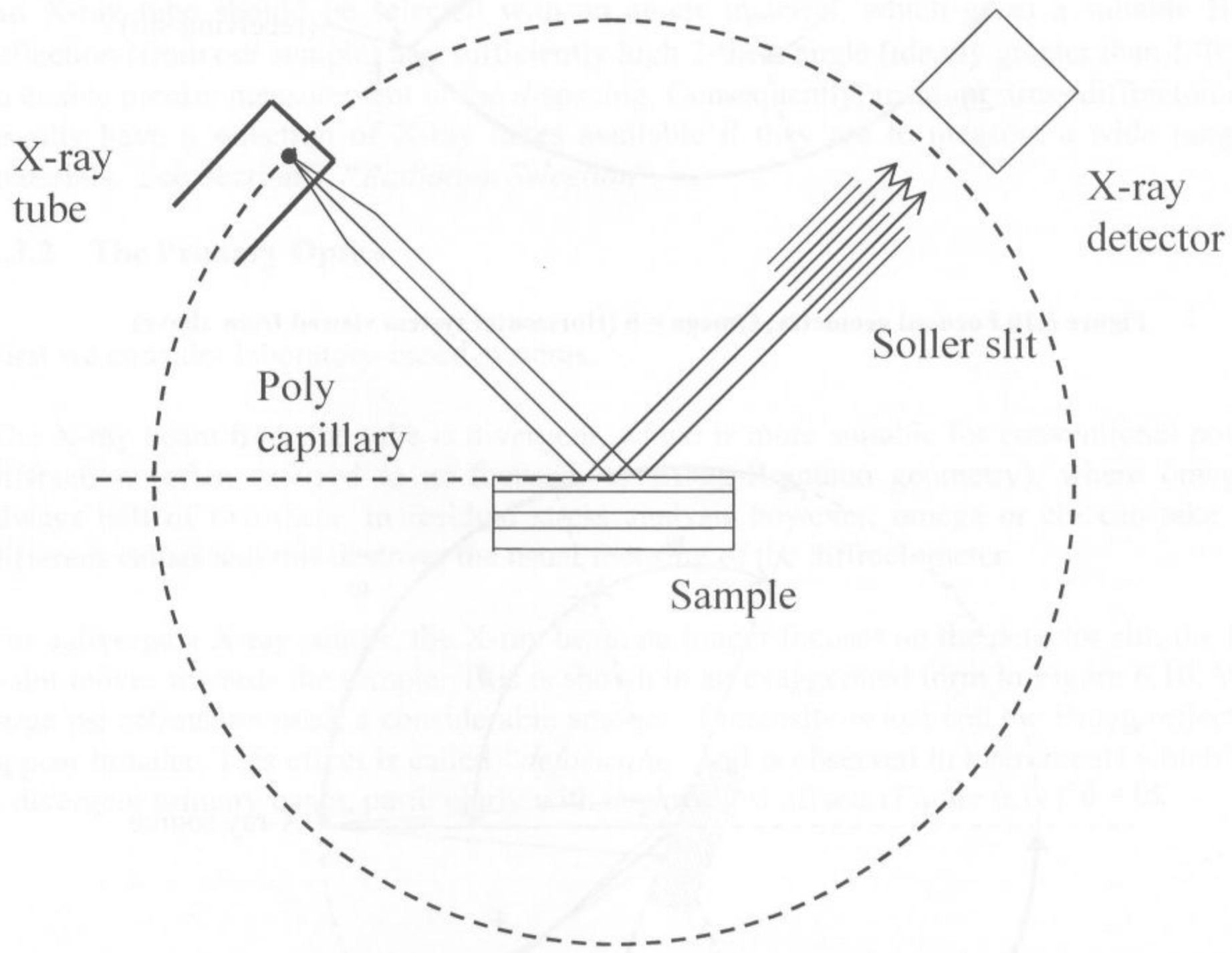

Figure 6.12 Poly-capillary, an X-ray "lightpipe", can be used with any wavelength

6.2.2.2 Mirrors

Mirrors are less common on residual stress machines as they are specific to a particular X-ray wavelength; usually copper K-α. An X-ray mirror is a shaped, synthetic crystal with a graded *d*-spacing which produces a very intense and parallel beam of X-rays, as shown in Figure 6.13.

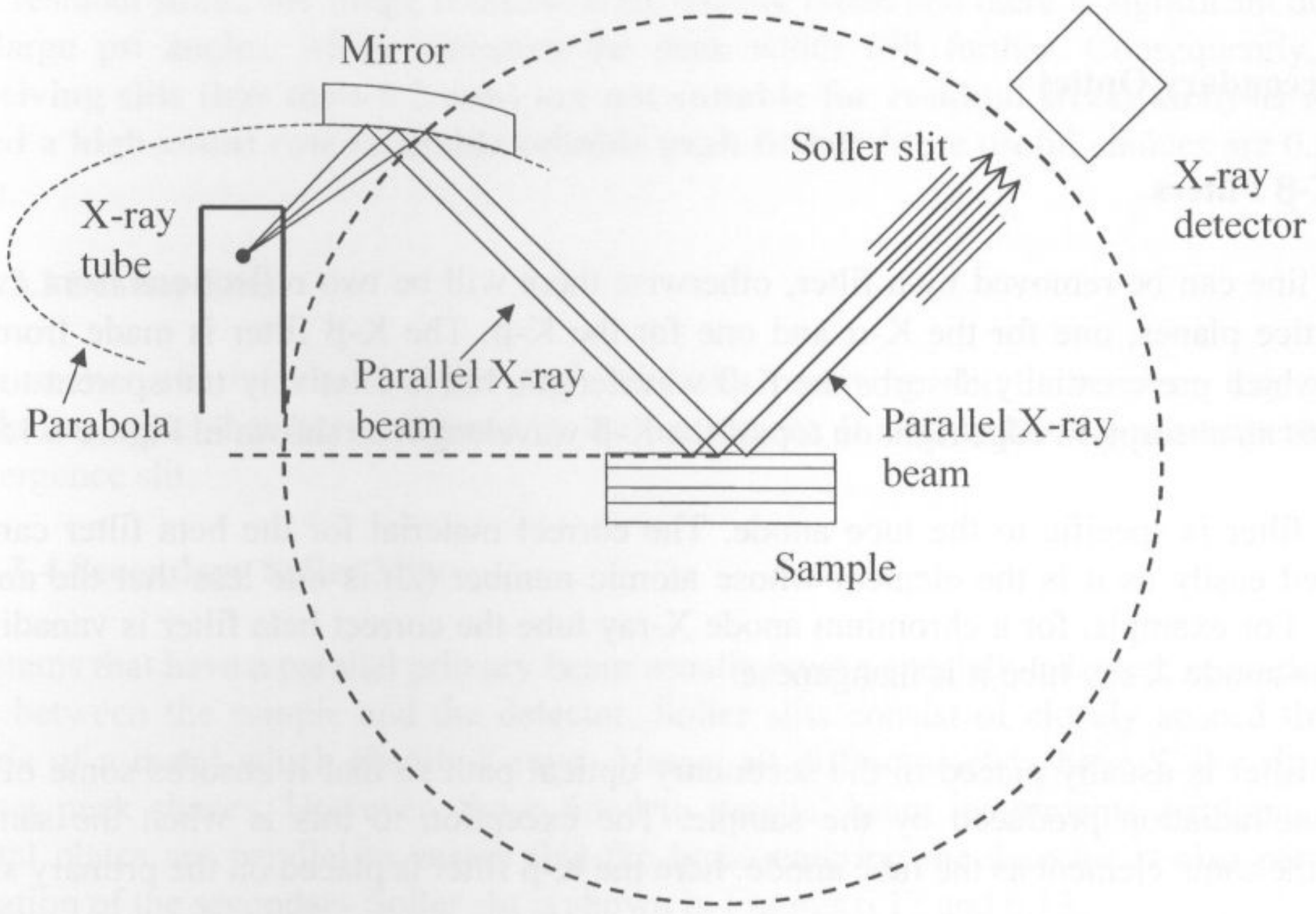

Figure 6.13 Schematic of an X-ray mirror

6.2.2.3 Slits

In most laboratory based systems the area of the sample which is irradiated is controlled by a slit in the primary optical path, called the divergence slit. Its aperture is measured in degrees: typical sizes are 1° and ½°. The divergence slit is combined with a mask, which limits the irradiated area laterally, as shown in figure 6.14.

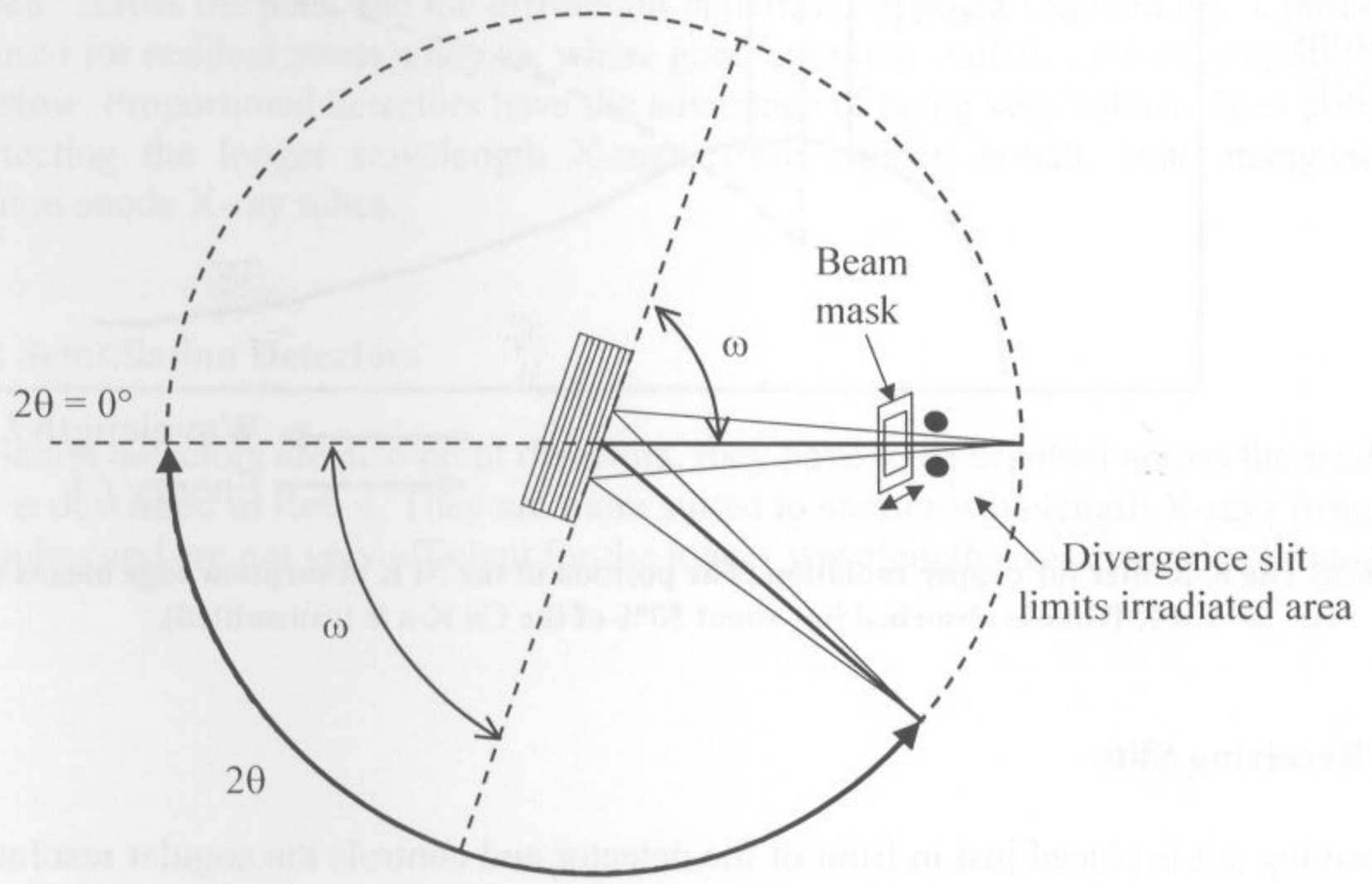

Figure 6.14 Primary divergence and beam mask-slit limits irradiated area with a divergent X-ray source (Horizontal system viewed from above)

6.2.3 Secondary Optics

6.2.3.1 K-β Filters

The K-β line can be removed by a filter, otherwise there will be two reflections from every set of lattice planes, one for the K-α and one for the K-β. The K-β filter is made from an element which preferentially absorbs the K-β wavelength, but is relatively transparent to the K-α. It has an absorption edge right on top of the K-β wavelength as shown in Figure 6.15.

The K-β filter is specific to the tube anode. The correct material for the beta filter can be determined easily as it is the element whose atomic number (Z) is one less that the anode material. For example, for a chromium anode X-ray tube the correct beta filter is vanadium, for an iron anode X-ray tube it is manganese.

The K-β filter is usually placed in the secondary optical path so that it absorbs some of the fluorescent radiation produced by the sample. The exception to this is when the sample contains the same element as the tube anode: here the K-β filter is placed on the primary side.

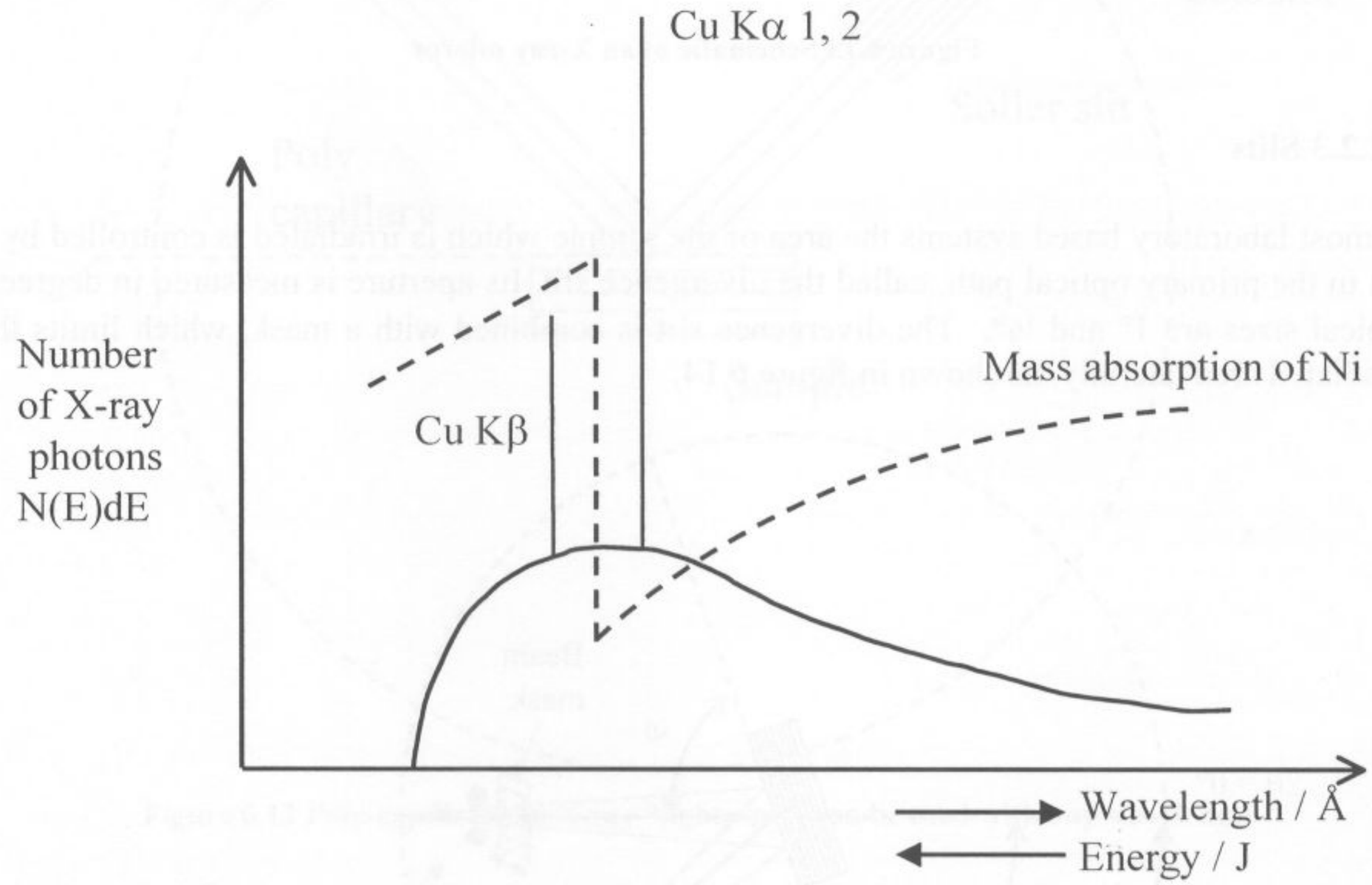

Figure 6.15 The K-β filter for copper radiation (The position of the Ni K absorption edge means that the Cu K-β line is absorbed but about 50% of the Cu K-a is transmitted).

6.2.3.2 Receiving Slits

The receiving slit is placed just in front of the detector and controls the angular resolution. Its aperture is measured in millimetres. A wide receiving slit will give poorer resolution but a higher count rate. Conversely, a narrow receiving slit will give better resolution but a much lower count rate.

For residual stress, the Bragg reflections are usually broad and there is significant defocusing at large psi angles, which increases the peak width still further. Consequently, **narrow receiving slits (less than 0.2 mm) are not suitable for residual stress analysis where we need a high-count rate to enable reliable peak fitting.** More useful choices are 0.3 and 0.4 mm.

6.2.3.3 Scatter Slits

The scatter slit is (usually) placed behind the receiving slit; it removes any unwanted radiation, which has been scattered by the instrument. It usually has the same aperture as the divergence slit.

6.2.3.4 Secondary Soller Slits

Systems that have a parallel primary beam usually have a specially adapted, secondary, Soller slit between the sample and the detector. Soller slits consist of closely spaced thin plates, made of a metal which absorb X-rays. Almost all diffractometers have Soller slits, to give better peak shapes. However, those fitted to parallel beam instruments are longer and the metal plates are parallel to ensure that the beam entering the detector is also parallel. The location of the secondary Soller slit is shown in Figures 6.12 and 6.13.

6.2.4 Detectors

There are several different types of detector which are fitted to residual stress diffractometers.

6.2.4.1 Proportional Detectors

These are "point" detectors; their design is described in Ref. 4. This type of detector has to be "scanned" across the peak and the diffraction pattern is collected sequentially. Consequently, when used for residual stress analysis, where good counting statistics are a necessity, they are rather slow. Proportional detectors have the advantage of being very robust. They are suitable for detecting the longer wavelength X-rays, from copper, cobalt, iron, manganese and chromium anode X-ray tubes.

6.2.4.2 Scintillation Detectors

Scintillation detectors are also point detectors; they have to be scanned across the peak. Their design is described in Ref. 4. They are more suited to shorter wavelength X-rays from copper anode tubes and are not very efficient for the longer wavelengths, for example chromium.

6.2.4.3 Position Sensitive Detectors (PSDs)

PSDs are "line" detectors. They consist of a wire or fluorescent screen that enables an angular "window" of data (usually about 15° 2-theta) to be collected simultaneously. They are particularly good for residual stress analysis where good quality data is required, quickly, over a relatively short angle range.

6.2.4.4 Area Detectors

Using an area detector a large section of the diffraction cone can be collected simultaneously. An example is shown in Figure 6.16. Area detectors are bulky, rather fragile and easily saturated by sample fluorescence, particularly as the K-β filter has to be placed in the primary optical path. However, it is possible to see any variations in intensity around the diffraction cone, which gives valuable information about grain size and texture (see examples in Figure 6.17).

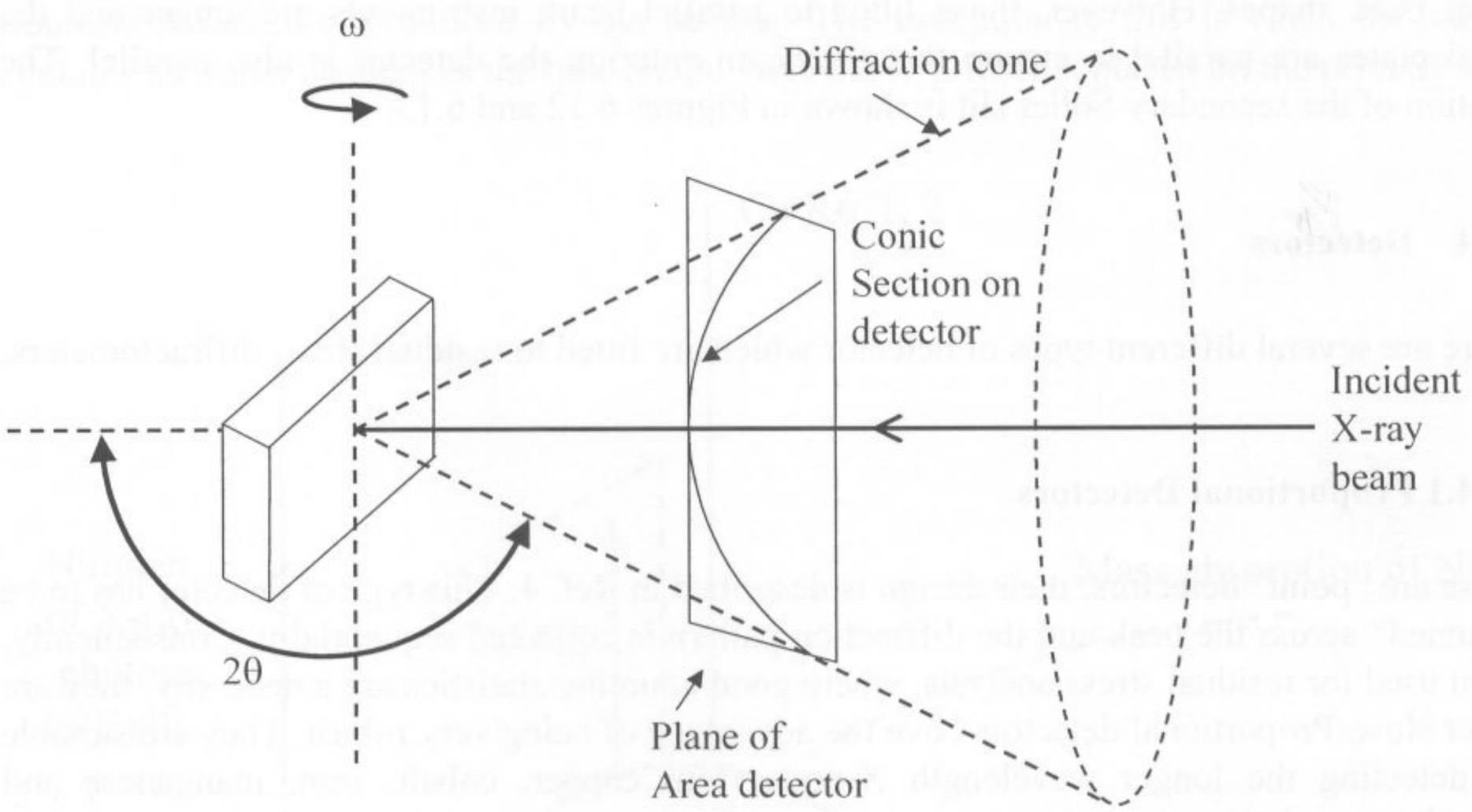

Figure 6.16 Conic section where the cone of the diffracted X-rays intersects the flat area detector

6.2.5 Secondary Monochromators

Point detectors (proportional and scintillation) can be fitted with secondary monochromators. The monochromator (a graphite crystal) transmits only the K-α radiation; the K-β, sample fluorescence and white radiation are blocked. Monochromators can be fitted to systems with either parallel or focused optics.

Obviously, not all of these components are compatible. Table 6.1 gives suitable combinations for parallel beam and focused system.

Table 6.1 Suitable combinations for focusing and parallel beam systems

	Primary Optics	**Secondary Optics**
Focusing systems	Divergence slit & beam mask	Receiving & scatter slits
Parallel Beam Systems	Poly-capillary or mirror	Secondary soller slits

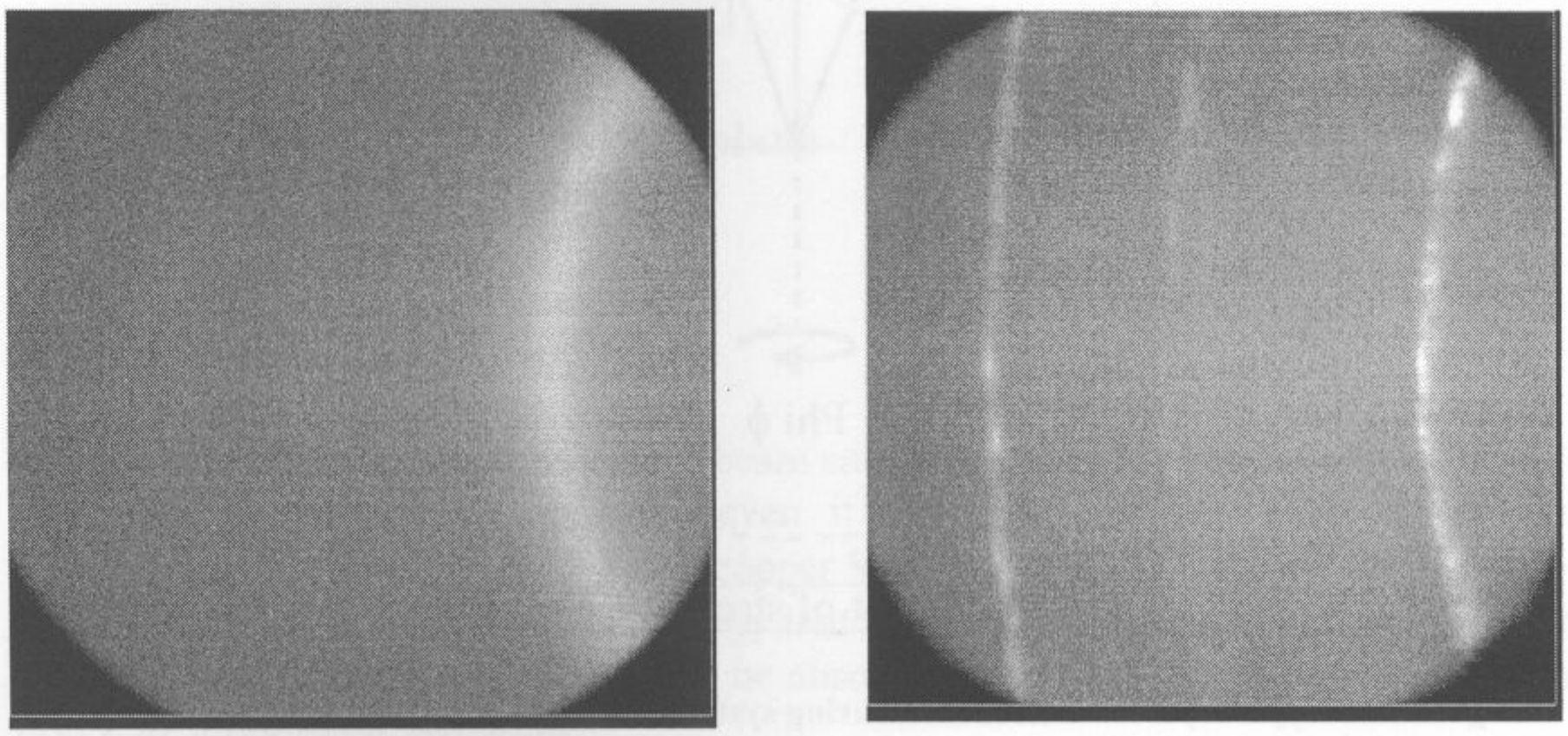

(I) (II)

Figure 6.17 Debye diffraction rings collected using an area detector

(I) Diffraction pattern from a sample of ferrite: here the grains are small & the intensity is even around the ring.

(II) Diffraction pattern from a sample of aluminium; here the grain size is larger, as can easily be observed from the uneven intensity distribution around the Debye ring. It is possible to integrate the intensity around a small section of the ring to reduce (but not eliminate) these intensity variations.

6.3 Portable Systems

These are much simpler than the lab-based systems. A portable diffractometer is shown schematically in Figure 6.18. The X-ray path length is much shorter than in a laboratory based system.

Figure 6.18 shows a schematic representation of a typical portable stress system. The instrument shown is an omega diffractometer. Combined chi and omega diffractometers are also available. The sample remains stationary, only the assembly carrying the tube and

detectors moves, allowing the machine to accommodate very bulky samples, or even to be placed onto a large structure.

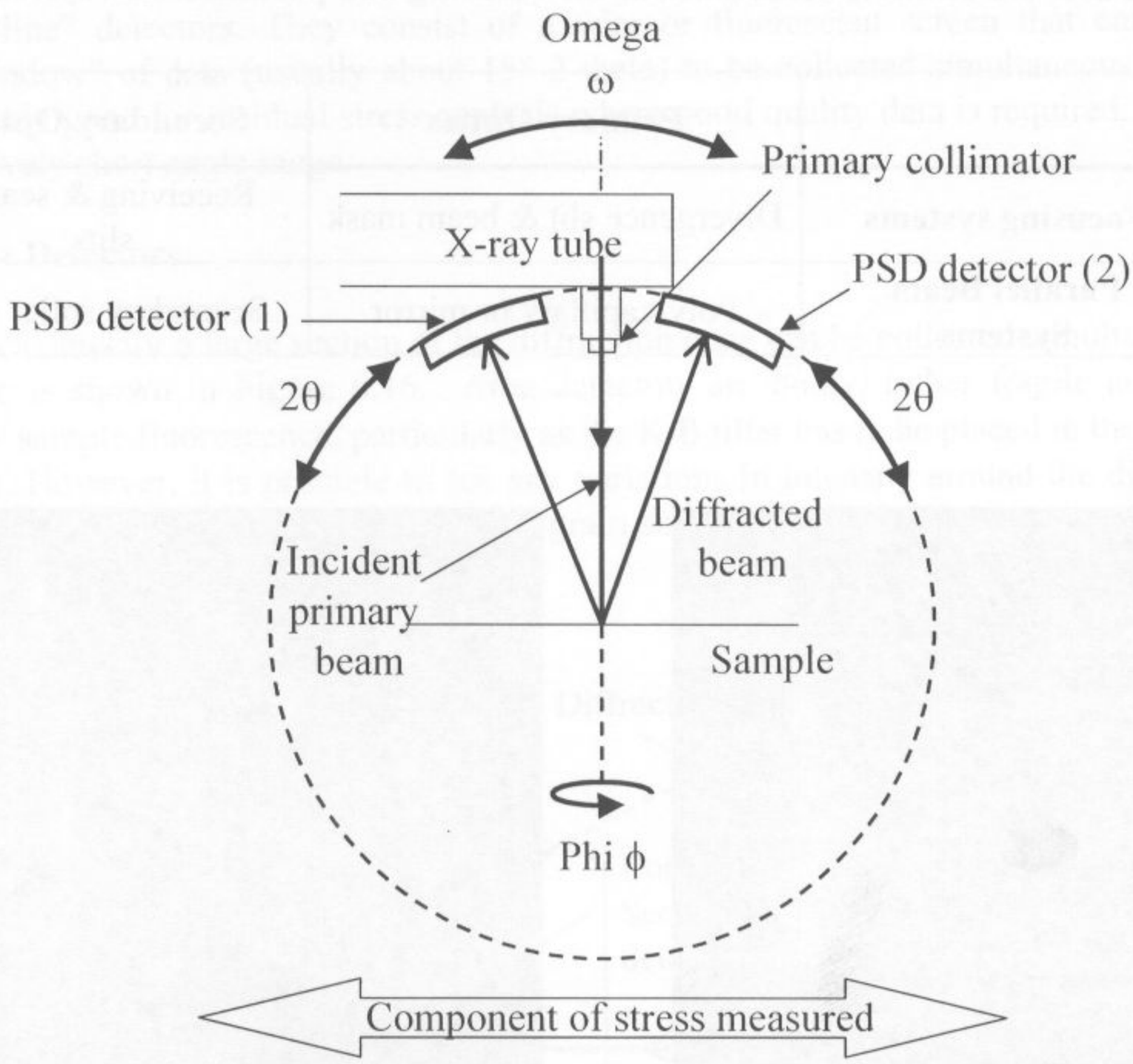

Figure 6.18 Typical portable stress measuring system shown in omega configuration

6.3.1 Primary Optics

6.3.1.1 Collimators

Portable stress diffractometers usually have a set of interchangeable collimators, either round or rectangular that limit the irradiated area.

6.3.2 Secondary Optics

Usually, there are just two small PSD type detectors, with a slot on each detector for installing a beta filter. Most portable systems have two detectors, which intercept opposite sides of the diffraction cone, enabling two psi offsets to be measured simultaneously.

6.4 Sample Positioning

It is important that the sample is placed exactly on the axis of rotation or the irradiated area will vary with psi. All instruments have devices to enable this.

Portable systems have a small pointer attached to the goniometer head which touches the sample and then retracts a known distance.

Laboratory based systems usually incorporate a dial gauge.

7 Radiation Selection

The choice of X-ray tube anode and therefore the wavelength of the incident X-rays is critical for the measurement of residual stress.

The following criteria must be considered:

- **Sample fluorescence**
- **Diffraction angle**
- **Choice of crystallographic plane**

7.1 Sample Fluorescence

If the K-α_1 component of the incident beam causes the sample to emit its own fluorescent X-rays, the radiation is not suitable, even if the instrument is fitted with a secondary monochromator. An example is using copper K-α radiation with an iron sample. The copper K-α radiation has a slightly higher energy that the iron K-α absorption edge. The copper K-α radiation is exactly the right energy to be absorbed by the iron atoms and is then emitted as iron K-α, fluorescent radiation.

Fluorescence produces a very high background and consequently poor peak-to-background ratio. This can be dramatically improved by using a secondary monochromator, which will remove the fluorescent radiation before it enters the X-ray detector. However, as most of the incident X-ray beam is being absorbed by fluorescence, the penetration depth into the sample surface is very small and is insufficient for a representative stress measurement of a bulk sample.

Usually, a longer wavelength is selected, as this radiation will not have sufficient energy to cause fluorescence. For an iron sample a good choice would be a chromium anode X-ray tube. The longer wavelength (less energetic) chromium K-α radiation actually penetrates further in to an iron sample than the more energetic copper K-α.

7.2 Diffraction Angle, 2-Theta

The changes in the *d*-spacings due to the strain in the sample are very small, typically in the third decimal place. We need to select an X-ray wavelength that will give a reflection, from our sample, at the highest possible 2-theta angle.

According to Bragg's Law the *d*-spacing from which a diffraction peak is obtained using a particular incident wavelength is a function of sin θ, and obviously, the relationship is not

linear. The change in position of a diffraction peak $\Delta\theta$ (and hence $\Delta 2\theta = 2\Delta\theta$) when there is a change in *d*-spacing, Δd, is obtained by differentiating Bragg's Law, which gives

$$\frac{\Delta d}{d} = -\Delta\theta \cot\theta \qquad \textbf{14}$$

At high 2-theta angles small changes in the *d*-spacing (like those due to strain) will give measurable changes in 2-theta, although the peak shifts are still only a few increments of a degree. At low angles the difference will be too small to be measured with any degree of precision.

Ideally, the radiation source should be selected to give a reflection at a Bragg angle greater than 130° 2θ. However, though not ideal, it is possible to use reflections which are as low as 125° 2θ. **Using reflections with 2-theta angles of less that 125° is not recommended**.

A wavelength should also be chosen that does not give a reflection too close to the high 2-theta limit of the instrument. Care must be taken to record the whole diffraction peak down to the background at both the upper and lower angular ranges.

7.3 Choice of Crystallographic Plane

Different crystallographic planes vary in their deformation mechanisms and give different responses for both elastic (residual stress) and inelastic strain (line broadening). Measurements made on different crystallographic planes are generally not comparable. Also, measurements made with different radiations may not be comparable due to the differing penetration depth of the X-ray beam into the sample, this is more an issue where steep stress gradients are present: see Section 5.4 for more details on penetration depths.

If it is suspected that the sample is textured, select the reflection with the highest multiplicity as this may reduce oscillation in the $\sin^2\psi$ plot. If the sample has a large grain size it may also help to select the reflection with the highest multiplicity.

For accurate comparisons with previous data/measurements it is useful to check which planes have been used, historically, and if possible select the same ones.

Note: It is necessary to check the diffractometer alignment by measuring both a stressed and unstressed standard every time that the X-ray tube is changed or replaced.

Table 7.1 shows recommended X-ray tube and {hkl} plane combinations for a variety of materials.